



# Knee UHMWPE Arthroplasty Optimization of Volumetric Wear Predictions with Improvements in Linear Abrasion. First Part



## Francisco Casesnoves\*

PhD Engineering, MSc Physics-Mathematics, Medical Doctor, Physician. Independent Bioengineering Laboratory. IAAM member, International Association of Advances Materials, Sweden. Uniscience Global Scientific member Wyoming USA.

**Submission:** May 05, 2026; **Published:** May 21, 2026

**\*Corresponding author:** Francisco Casesnoves, PhD Engineering, MSc Physics-Mathematics, Medical Doctor, Physician. Independent Bioengineering Laboratory. IAAM member, International Association of Advances Materials, Sweden. Uniscience Global Scientific member Wyoming USA. casesnoves.research.emailbox@gmail.com

### Abstract

Following up with previous advance series, volumetric wear predictions for alloy-UHMWPE Total Knee Arthroplasty (TKA) are simulated-optimized for classical Archard's model (AM). Mathematical algorithms for Integer and Integral volumetric wear are explained. 2D-3D Imaging-processing computational simulations software designed with Graphical Optimization and Interior Optimization techniques. For [1-5] Million Cycles (Mc) results in Volumetric Wear, the numerical dataset and 3D simulations image-processing graphs are demonstrated. Second part shows improvements-review for AM Linear Abrasion. Applications in Biotribology/Biomaterials are presented.

**Keywords:** Total knee arthroplasty (TKA); 3D Simulations; Optimization; Linear Wear; Mathematical Model; Load; Sliding Distance; PE (Polyethylene); Wear Factor (WF)

**Abbreviations:** Archard's Model: AM; FE: Finite Elements method;  $K_{wear}$ : Wear Factor (WF);  $L_{wear}$ : Linear;  $V_{wear}$ : Volumetric Erosion; Mc: Million cycles; PE: Polyethylene (UHMWPE); TKA: Total Knee Arthroplasty; UHMWPE: ultra-high molecular weight polyethylene.

## Introduction and Objectives

Continuing in UHMWPE-TKA prostheses research line, this study focuses on TKA volumetric abrasive erosion computational predictions. Linear and volumetric wear predictions show significant magnitude differences [1.1-1.12, 2.1-2.32], Equations 1. TKA models are very specific as algorithmic-functions of, among others, anatomical, biomechanical, biodynamics, biotribological and bioenergy proper knee characteristics. Classically, Archard's model (AM) formula applied for TKA wear is based, for linear wear, on a straight-line sliding magnitude of the femur TKA-alloy condyle along the UHMWPE tibial-part of the prosthesis, Figure 1. For linear AM, sliding distance is an important magnitude, but considering that within the algorithm, load can be divided by contact surface, it could result nonlinear, unless the pressure magnitude is directly implemented. AM do not consider the TKA shear phenomenon, and that is a biotribology inconvenient, [1.1-1.3]. For AM, the linear and volumetric wear prediction calculations, consequently, differ in units and magnitudes,

Equations 1-3. AM algorithm-constant is a dimensional so-defined Wear Factor with proper dimensions, ( $\text{mm}^3 / \text{N m}$ )-note that for this study programming is set as ( $\text{mm}^3 / \text{N mm}$ ). Its magnitude order differs along the literature, around  $10 \exp(-9, \text{ or } -10)$  magnitude order, [2,3], provided is set as ( $\text{mm}^3 / \text{N mm}$ ). Fixed-bearing TKA and Rotating-bearing TKA show differences related to contact area [2.1-2.7]. This is an important difference between two types of TKA-tibial-plateau component. Contact areas are different, but numerical linear wear predictions with AMs do not differ significantly. Unicompartimental TKA constitutes a different special TKA implant.

There are more differences between volumetric and linear wear and difficulties in their determination for TKA wear standards. One important characteristic of TKA along the extensive literature is the large variety of methods, biotribology laboratory apparatus, algorithms, units to present results, and ISO standards [2.6]. Here it is set the most important hurdles to understand and compare the

amount techniques and results. The most frequently units to present results are mm/Mc for linear wear, and mm<sup>3</sup>/Mc for volumetric one. The wear magnitudes and rates differ in literature and laboratories for two main reasons: (1) the large variety of testing apparatus and methods, (2) the large variety to communicate/measure results. Namely, wear per Mc (mm), wear per year (mm), wear per Mc (mg), wear per year (mg), and others. When the study is *in vivo*, wear is usually expressed in mm/year, what is common is the polyethylene density approximately equal to water, about 0.96 mg/mm<sup>3</sup>. One reason for that is the archive of the patient history, that gives the number of TKA implantation years, and the wear of the implant is related to that lifetime. Additional complementary dataset and further reading can be found at [2.1-2.7]. Conversion of units: although it seems complicated, some techniques can be used to convert undesirable units in any publication results into other ones more convenient if it is the case-approximately. When linear/volumetric results are shown in erosion/year, (it could be mm, mm<sup>3</sup>, or mg), there are references to calculate approximately the number of Million Cycles (Mc) per year [2.5]. In doing so, an approximation is got to convert mm/year into mm/Mc through statistics of average number of Mc per year [2.5]. For instance, if the results are shown in mg, it is easy to convert taking into account that UHMWPE density is approximately the water one, about 0.96 mg/mm<sup>3</sup>. ISO norms show kind of like hurdles to evaluate the literature results. ISO norms are regulated but profuse. When comparing experimental and simulation results/datasets it is rather difficult, even if the studies have set the same ISO norms, [2.6]. Different apparatus usage constitutes another difficulty. TKA biotribology laboratories use a large amount of different manufactured machines to get trustworthy results [2.5-2.6]. The apparatus differs in output units, design, or mechanical methods to measure erosion. As a result, it is a must to study all those before interpret linear or volumetric TKA erosion dataset. Finally, different computational methods and models are applied in the literature studies. The standard method for TKA erosion research is FE. However, the FE variety methods is large, and the algorithms implemented within FE calculations differ. The FE computational systems are varied, for example, Abaqus or Matlab, [2.1-2.7].

Therefore, the rationale of this study is to get an initial precise volumetric wear for UHMWPE TKA. AM is classical, but still widely used, (specially for FE calculations) and Cross-Shear model (not selected for this study), is more recent and in general gives higher erosion magnitude orders, e. g., [2.1-2.3]. It is not an objective of the research to assert any arguments to consider totally superior/inferior any of those models. Instead, the aim is explained and demonstrate AM algorithms, precision, predictions, and research options when using AM. What is biomechanically clear, Figure 1, is that the sliding of the TKA can be approximated, following AM, as straight line-curve, but anatomically it does not happen. The method used in Graphical and Interior Optimization software, with specific algorithms. The designed programming is precise and the graphs are intended be sharp and illustrative.

### Objectives

Therefore, objectives are mainly two. First and foremost, to design software engineering for computational-simulations and optimization of volumetric AM. Secondly, to review and improve previous studies for AM linear wear. Complementary biomechanical and biodynamics applications are explained.

In summary, volumetric wear simulation-optimization research was done with the classical Archard's model. Computational intelligence software was designed for AM algorithms. Improvements for AM linear wear were included. 2D-3D imaging-processing graphical and interior optimization results agree the most literature results for these models in linear wear. TKA applications are briefed.

### Archard's Model (AM) Volumetric Concepts and Algorithms

This section deals with the main AM algorithms for computational implementation. Mechanical parameters and units are detailed.

### The Basic Integer AM Model Volumetric Algorithm

For TKA volumetric wear, an integer algorithm was developed based on AM, Equation 1. In the literature, several AM varied-algorithms have been presented [2.1-2.12]. Therefore, in this study, the basic volumetric algorithm-model from [2.3-2.11], applied and analyzed mathematically by Author, reads,

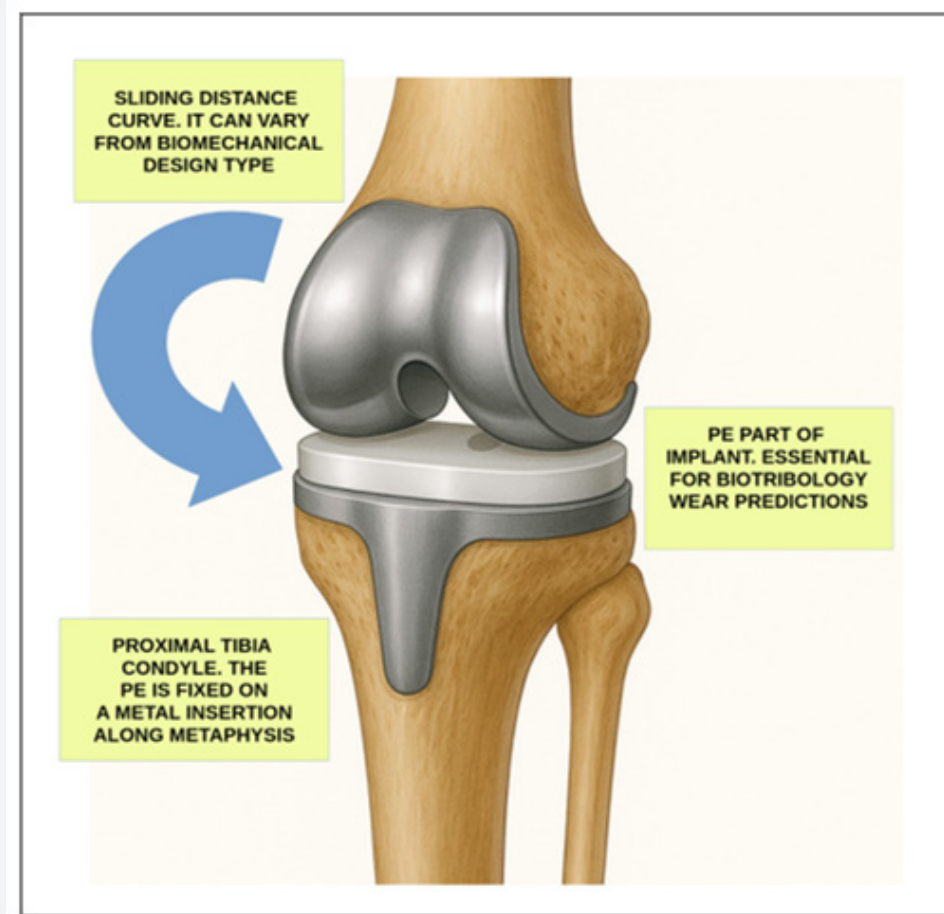


Figure 1: [Google free-usage images, drawn-modified and complemented by Francisco Casesnoves]. The sketch is completed with main parts of TKA. Inset, the most important anatomical parts are marked. Note that the femur condyles are made in steel-alloy, and the tibial plateau is polyethylene. More sketches that illustrate the TKA biomechanics can be found at [8.5]. The biomechanical analysis, to demonstrate the basis of the TKA models anatomical is shown inset. The natural curvature of the tibial plateau-the upper surface of the bone-is asymmetrical, with distinct shapes for the medial (inner) and lateral (outer) sides. These differences are critical for natural and TKA knee stability, biodynamics and biomechanics. For example, at natural anatomy of curvature the tibial plateau is divided into two articular surfaces with opposing geometries: medial tibial plateau: It is concave in both the sagittal (front-to-back) and coronal (side-to-side) planes. This 'bowl' shape, not seen at sketch, provides a stable seat for the larger medial femoral condyle. Lateral tibial plateau: It is generally convex in the sagittal plane and flat to slightly convex in the coronal plane. This natural 'dome' shape, situated slightly higher (more proximal) than the medial side, allows for the complex rolling and gliding motions of the knee. Natural and TKA knee forces decomposition: the vertical load, over the bent tibial plateau surface, decomposes into two forces. One lateral, that causes shear in the prosthesis, and a second perpendicular to the plateau surface. Therefore, although in this study this is not considered for AM, it is clear that mechanical shear occurs during movement. Classical AM model considers a sliding path exclusively along the AP or PA directions, omitting the lateral-shear forces/displacements.

$$V_{volumetric} = A \times L_{wear} = A \times K_{wear-factor} \sum_{j=1}^N \left[ \sum_{i=1}^n p_i |v_i| \Delta t_i \right]_j ;$$

[ 1. Casesnoves Bioengineering Laboratory. Algorithm-development-311]

where,

A: Contact area (mm<sup>2</sup>).

$V_{volumetric}$ : Volumetric abrasive wear (mm<sup>3</sup>).

$L_{wear}$ : Linear abrasive wear (mm).

$K_{wear}$ : Archard-Model: Wear Factor, standard ( $\text{mm}^3 / \text{N mm}$ ). Note: at figures values range of  $K_w$  are usually multiplied by  $10^{-3}$ .

$p_i$ : Pressure ( $\text{N} / \text{mm}^2$ ).

$v_i$ : Sliding discrete Velocity for discrete time increment ( $\text{mm} / \text{s}$ ).

$\Delta t_i$ : Discrete time interval (s).

$i, j$ : Summatory indexes. The  $[i]$  is for velocity variation within a cycle (n). The  $[j]$  is for cycles number (N).

The parameter intervals for software are set in real numbers large intervals, usually of 50-100 elements. However, this equation works at programming with that technique.

### The Integral AM Volumetric Algorithm

It is convenient, when experimental data or database available, to compute the algorithm as an integral-equation of first kind. Hence, taking trivial derivatives, integral, and limits for getting an integral form,

$$V_{wear} = A \times K_{wear} = A \times K_{wear\ factor} \times \sum_{j=1}^N \sum_{i=1}^M \left[ \int_0^{t_i} p |v| dt \right]_j ;$$

[ 2. Casesnoves Bioengineering Laboratory. Algorithm-development-311]

where,

A: Contact area ( $\text{mm}^2$ ).

$V_{wear}$ : Volumetric abrasive wear ( $\text{mm}^3$ ).

$L_{wear}$ : Linear abrasive wear (mm).

$K_{wear}$ : Wear Factor, for programs ( $\text{mm}^3 / \text{N mm}$ ). Note: at figures values range of  $K_w$  are usually multiplied by  $10^{-3}$  because of this change of units (generally  $K_{wear}$  is formulated ( $\text{mm}^3 / \text{N x m}$ ).

$p(t)$ : Instantaneous pressure ( $\text{N} / \text{mm}^2$ ). Function of time.

$v(t)$ : Instantaneous sliding velocity for integral. Function of time ( $\text{mm} / \text{s}$ ).

$dt$ : Differential of time during i-interval (s).

$i$ : Summatory index for time at every integral for a cycle (M).

$j$ : Summatory index for total cycles (N).

*The AM applied on TKA, volumetric integral form proof,*

*For one cycle,*

$$V_{w1} = A \times L_{w1} = A \times K_w p \times S;$$

Where  $S$  is sliding distance,  $p$  is pressure ( $p = \frac{F}{A}$ ), hence,

$$V_{w1} = A \times L_{w1} = A \times K_w \times \frac{F}{A} \times v \times t = \dots = K_w \times F \times v \times t;$$

*Therefore, providing v constant and taking derivatives for time variable,*

$$\frac{dV_{w1}}{dt} = K_w F v; \text{ or}$$

$$dV_{w1} = K_w F v dt, \text{ integrating,}$$

$$\int_0^t dF_{w1} = K_w \int_0^t F v dt, \text{ supporting instantaneous pressure and sliding velocity during one cycle,}$$

*Therefore, taking N cycles, ( $K_{wear}$  is Wear Factor), and integrating, conditioned to linear sliding,*

$$V_{wear} = K_{wear} \sum_{j=1}^N \sum_{i=1}^M \left[ \int_0^{t_i} |\vec{F}| |\vec{v}| dt \right]_j ;$$

[3. Algorithm developed by Casesnoves Bioengineering Laboratory Algorithm 3114]

where,

A: Contact area (mm<sup>2</sup>).

F: Load force (N).

V<sub>wear</sub>: Volumetric abrasive wear (mm<sup>3</sup>).

L<sub>wear</sub>: Linear abrasive wear (mm).

K<sub>wear</sub>: Wear Factor, for programs (mm<sup>3</sup>/ N mm). Note: at figures values range of K<sub>w</sub> are usually multiplied by 10<sup>-3</sup> because of this change of units (generally K<sub>wear</sub> is formulated (mm<sup>3</sup>/ N x m).

p(t): Instantaneous pressure (N / mm<sup>2</sup>). Function of time.

v(t): Instantaneous sliding velocity for integral. Function of time (mm / s).

dt: Differential of time during i-interval (s).

i: Summatory index for time at every integral for a cycle (M).

j: Summatory index for total cycles (N).

### Computational Dataset and Methods

This section deals with units, dataset, and computational methods for the study with AM.

#### Volumetric Wear Units Precision

Equation 4 shows the physics units system implemented for AM simulations. The units were used for AM, that is N, mm<sup>3</sup>, and mm<sup>2</sup>. Then, standard TKA wear units read,

*Standard literature units for Archard's model dimension equations,*

*For example,*

*Erosion in mm depth,*

$$L_w(\text{mm depth}) = K_w \left( \frac{\text{mm}^3}{\text{N mm}} \right) \text{Pressure} \left( \frac{\text{N}}{\text{mm}^2} \right) \text{Sliding Distance}(\text{mm});$$

as a result,  $L_w$  is in  $\text{mm}$ ,

Erosion in  $\text{mm}^3$  eroded material volume,

[4. Algorithm developed by Casesnoves Bioengineering Laboratory Algorithm 3114]

For volumetric AM, the second one is the primary method applied in this paper. That is Abrasive Volumetric Wear. Linear TKA knee-biotribology review/improvements are included at article second part.

#### Standard Abrasive Volumetric Wear Factor K<sub>w</sub> Magnitude

Given the fact that the number of laboratory apparatus, measuring systems, and hybrid studies are profuse, in the literature, there is not a total agreement for K<sub>w</sub> wear factor magnitude [2.3]. Figure 2 shows a double plot for K<sub>w</sub> and load related to Mc [1-5]. 2D GNU-Octave imaging processing multi-polynomial fit that describes the variation in function of K<sub>w</sub> variation and Million Cycles (Mc) [2.13-2.21] integer interval. Note: at figures values range of K<sub>w</sub> are usually multiplied by 10<sup>-3</sup>. Figure 2-upper shows AM linear wear related to Load-Mc parameters for [1-5] Mc. Figure 2-lower 6 presents AM volumetric wear related to wear factor K<sub>w</sub> for [1-5] Mc. Magnitude differences are significant.

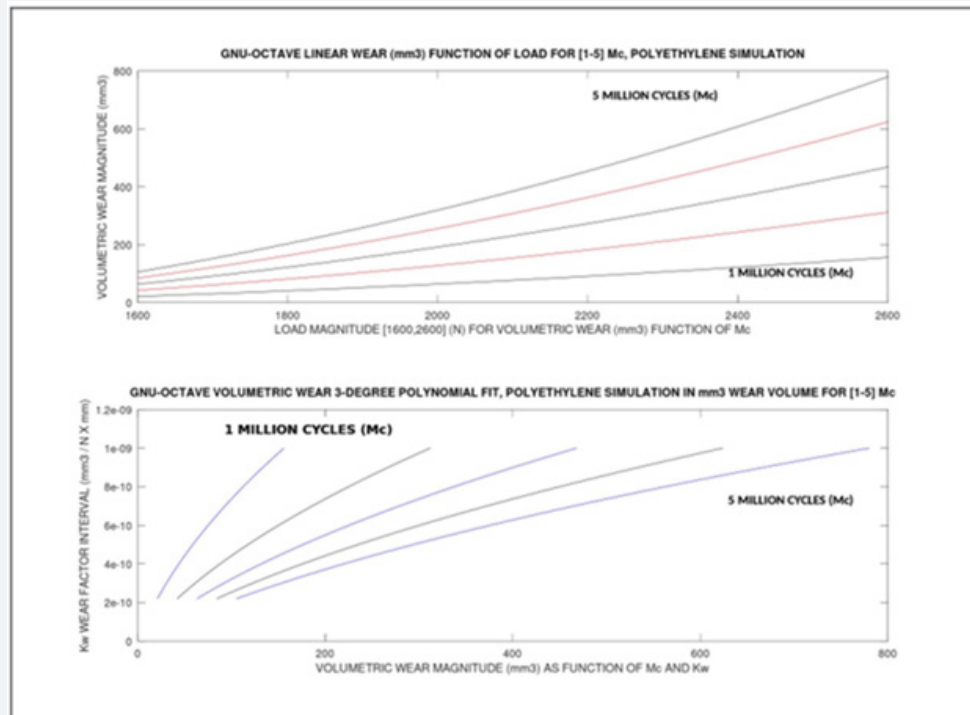


**Figure 2:** For parameters of Tables 1-2, example of polynomial fit for wear prediction in function of the load variation range of [ 1600,2600], (continuous), and Mc [1,5] (integer). It is clear the wear.

Figure 2 For magnitude variation related to increase of load and the Mc number. Previously the 2D imaging processing, a 3-degree polynomial fit was developed for every million-cycle graph-line type. [Casesnoves Bioengineering Laboratory Software 2025-M-3]. Also, for parameters of (Tables 1-2), example of polynomial fit for wear prediction in function of the variation range of [  $K_w \times 10^{-3}$  ], (continuous), and Mc [1-5] (integer). It is clear the magnitude variation related to increase of [  $K_w \times 10^{-3}$  ], and the Mc number. Note: at figures values range of  $K_w$  are usually multiplied by  $10^{-3}$ . Further references to contrast this dataset are generally in [1.1-1.12]. Previously the 2D imaging processing, a 3-degree polynomial fit was developed for every million-cycle graph-line type-different from upper Figure 2. This type of software is developed from Author's series of previous publications in hip prostheses wear and other computational contributions [1.5,3.1-3.6]. [Casesnoves Bioengineering Laboratory Software 2025-M-4].

### Computational Intelligence Dataset for Software

Dataset, (Tables 1-2), from literature is selected from parameter intervals at programs, because the commercial materials, TKA sizes, and Algorithm constants applied differ among authors, laboratories, testing apparatus, testing temperature, etc. As a result, it is necessary to choose those experimental datasets/magnitude-values which are commonly accepted in the literature. Therefore, the practical objective of the simulation-optimizations is to provide with large scale range that can be used to predict durability for all of those most important variants. Software is based on hip wear previous Author's contributions for hip wear programming design [3.1-3.6]. In those publications, both Tikhonov Regularization Theory and Evolutionary Algorithms were applied for hip optimization software-engineering. General additional biotribology database can be found at [3.7-3.17].

### Average Contact surface Magnitude

For volumetric wear, it is not necessarily needed for this kind of methods. That is a parameter interval rather difficult to implement within programs, both in Matlab and GNU-Octave. For both models in this study, the intervals published in [1.4] are set (Tables 1-2).

**Table 1:** Selected Dataset used for simulations and optimization software. [references-numeration-7-8]. Disclaimer: some variants were applied for trial programs and images. Note: at figures many times values axe-range of  $K_w$  are multiplied by  $10^{-3}$ .

SELECTED STANDARD DATASET USED FOR AM VOLUMETRIC AND LINEAR COMPUTATIONAL SIMULATIONS			
PARAMETER AND UNITS	INTERVAL OR MAGNITUDE SOFTWARE IMPLEMENTED	REFERENCES	PRECISION
LOAD (N)	[2000,2300-2600] Generally [2000,2600]	[1.1, 1.5, 11, 21, 21.1, 21.2]	Standard magnitude, usually agreed by most authors. The most implemented interval is [2000,2600]
SLIDING DISTANCE (mm)	60	[2.10]	ISO Standard, it varies according to studies.
KW (mm <sup>3</sup> / (N x mm))	[2.20 x 10 <sup>-7</sup> , 10 <sup>-6</sup> ] [Note: at figures values range of Kw are usually multiplied by 10 <sup>-3</sup> because all the units are set in mm at software]	[2.3, 2.21]	The constant KW has different values in literature. It is implemented an interval that comprises most published magnitudes.
LOAD SURFACE (mm <sup>2</sup> )	[ 1000, 2300-2600]	[2.21, 2.21.1, 2.21.2]	This varies significantly according to several publications.
CYCLES NUMBER (in M (millions)) notation standard: Mc	[ 1, 5] image-processing is shown for [ 2, 5] Mc and [1, 5] Mc	[2.1-2.11, 2.13-2.32] [articles, 2.1-2.10]	It is presented, usually, in most books and papers dataset from 1 M to 5 M. Most authors show predictions and calculation testing for 1-5 Mc.
IMPLEMENTED: KW (mm <sup>3</sup> / (N x mm)) x 10 <sup>-3</sup> according to (8.3)	[ 2.20 x 10 <sup>-10</sup> , 10 <sup>-9</sup> ] See Figures 1-8	[2.3]	KW has different magnitude according to authors, [3], and some researchers propose values of KW, for example [21].
Poisson ratio and Elastic modulus, Density, for UHMWPE	<b>NOT IMPLEMENTED, EXCLUSIVELY ILLUSTRATIVE UHMWPE: Young's modulus 463 MPa, Poisson' ratio 0.46, density 960 kg/m<sup>3</sup> [21i].</b>	[2.21]	N/A for the algorithms which are programmed.

**Table 2:** Selected Dataset used for simulations and optimization software. Disclaimer: some variants were applied for trial programs and images. Note: at figures many times values axe-range of  $K_w$  are multiplied by  $10^{-3}$ .

AM SOFTWARE-ENGINEERING PARAMETER-INTERVALS LITERATURE REFERENCES		
PARAMETER AND UNITS	REFERENCES FOR SOFTWARE IMPLEMENTED	EXTENSIONS
LOAD (N)	[2.1, 2.11, 2.21, 2.21.1, 2.21.2]	Standard magnitude, usually agreed by most authors. It is important to set at patterns a magnitude interval as wider as possible to get trustful comparisons/predictions.
SLIDING DISTANCE (mm)	[2.10]	ISO Standard, it varies, from [40,80] mm usually. For CSM is generally longer.
Wear Factor KW (mm <sup>3</sup> / (N x mm))	[2.3, 2.21]	The, [8.3], range is applied for software. Recalling to note the difference between wear factor (AM), dimensional, and wear coefficient (Cross-S-shear Model), a dimensional.
LOAD SURFACE (mm <sup>2</sup> )	[2.21, 2.21.1, 2.21.2]	[8.1] shows standard coronal size and loads.
CYCLES NUMBER (in M (millions)) notation standard: Mc	[2.1-2.11, 2.13-2.32]	It is presented, usually, dataset from 1 Mc to 5 Mc. In the literature, the most usual is show a range [1,5] Mc.
Wear Factor IMPLEMENTED: KW (mm <sup>3</sup> / (N x mm)) x 10 <sup>-3</sup>	[2.3]	It is considered sufficient confident interval that comprises almost all authors publications.
Poisson ratio and Elastic modulus for UHMWPE	<b>NOT IMPLEMENTED, EXCLUSIVE ILLUSTRATIVE, UHMWPE: Young's modulus 463 MPa, Poisson ratio 0.46, density 960 kg/m<sup>3</sup> [ 8.21 ].</b>	N/A for the algorithms which are programmed.

## Benchmark polyethylene model (optional)

For volumetric wear, it is optional. There are variations for the TKA size in literature about laboratory studies. However, the size used for simulation software implementation was the most standard one, [2.1-2.3, 3.18]. That is, 78.2 x 44.2 mm the total coronal dimension, from that magnitude the contact surface was approximated-calculated. That size is according to ISO, and it is noteworthy to consider that there are ISO variants.

## Sliding Distance (SD)

Sliding distance recommended by ISO is about 80 mm [2.10]. However, it was set [60,80] mm, taking into account differences between prostheses sizes, [2.12].

## Load Magnitude Interval

This is a magnitude convergence point for most of studies. The most usual assumed magnitude by majority of investigations [2.21, 2.21.1-2.21.2]. For example [2.2, Table 2, page 63] gives an overview of the changes of loads and gaits from normal walk to down stairs/ramp. From this Table and setting a patient average weight of 75 kg, the interval of loads that comprise approximately walk, stairs and climb down/up, etc, can be deducted. Usually, then, is [1600, 2600] N interval. Here it is taken a maximum interval of [2000,2600] N in most simulation-programs. Other Authors, [2.21], apply a maximum load of 3000 N. That is not considered for this study, because those loads are not for usual patient walk. That is, walk to down stairs in a normal patient activity happens during a few minutes in general.

## Standard Unit System

The Volumetric Wear standard TKA erosion AM units used in literature, most times, are mm<sup>3</sup> of eroded material or mm depth of erosion along contact surface. When studies are in vivo or provided with cadaveric history, the Linear Wear is given in mm/year. It is not an objective of this study to discuss the optimal unit system. Instead, the image-processing and numerical data is expressed in mm<sup>3</sup> volume to bring for user the choice to compare dataset appropriately, [2.3,2.11]. For passing erosion magnitude/year to mm<sup>3</sup>, it is taken into account the average Mc for a year, [2.16], which is about 2 Mc/year-precisely, that is a rather difficult parameter since variations among patient groups, countries, and laboratories are high. The physics dimension equations for AM Linear and Volumetric Abrasive Wear are explained in Equation 4. Tables 1-2.

## Volumetric Wear Dataset

Table 1 shows dataset implemented parameters for volumetric AM wear

## Computational intelligence Software

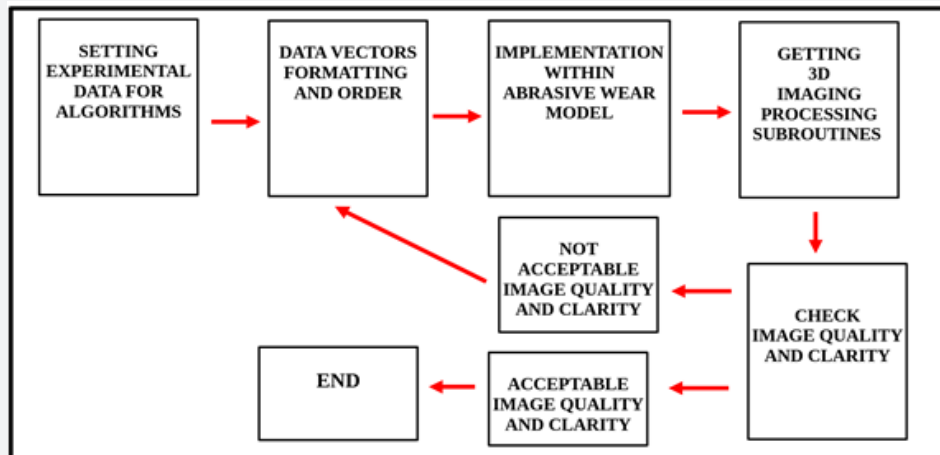
The most important parts of the software are mainly two. Both are difficult. The first one is the matrices setting withing patterns and their congruence for mathematical operations. The second hurdle is the 2D-3D imaging processing subroutines setting, because not any order for getting an accurate image is efficacious when obtaining the 2D-3D image.

## Programming Structure

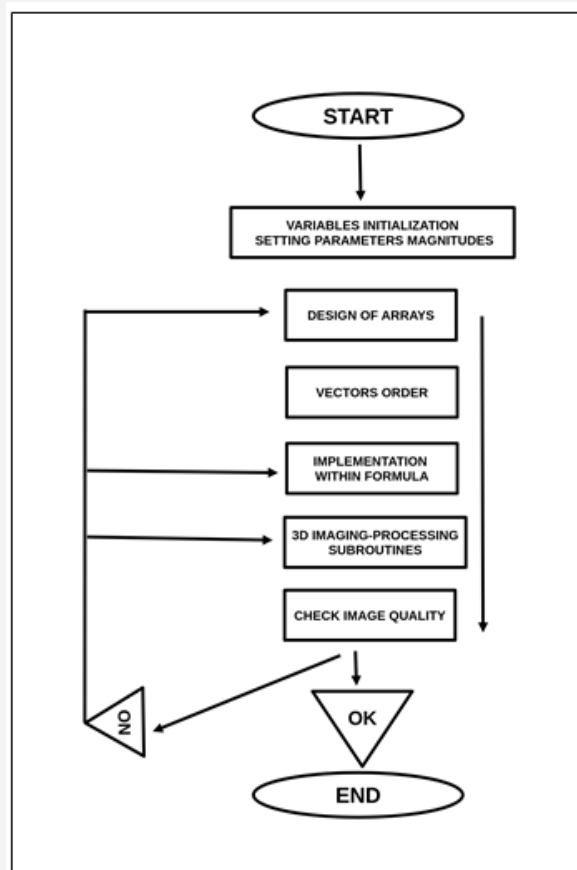
It was developed, Sketchs 1-2, software programming mainly from previous experience in hip wear models [2.33-2.34]. Systems used were Matlab 2023 and GNU-Octave 8.1.0. For programming algorithms 1-2, the difficulty was the matrices congruency and the loops for arrays. Figure 3 shows the software pattern to check image-processing quality. Sketchs 1-2 explain the basic programming structure.

## 7 AM Volumetric Wear Results

Figures 2-5 shows the AM volumetric wear for 2-5 Mc, GNU-Octave and Matlab imaging-processing system. Matlab image-processing quality and tools are better, but GNU-Octave is acceptable. The minimum Mc is chosen 2 because it corresponds approximately to 1 year erosion in literature, Table 2. However, this criterion, [2.16], is not completely confirmed in literature, and constitutes an approximation. Cycles number per year depends on multiple factors, e. g., activity, country, work, personal habits, sex, etc.



**Sketch 1:** Basic programming flow chart that shows the software pattern to check image-processing quality. The foremost essential is to gather trustful experimental data. Secondly important in those programs are the arrays and their implementation within the algorithm. The experimental dataset can be vectorized in many forms, and the selection of the optimal one is crucial. If the dataset-vectors are not conveniently re-arranged and set at the 3D imaging processing subroutines, the resulting image could not be acceptable. There are image-processing tools in Matlab and GNU-Octave to improve image clarity and sharpness. [Casesnoves Bioengineering Laboratory Software 2025-M-4].



**Sketch 2:** Complementary and basic programming flow chart. The most important of those programs are the arrays and their implementation within the algorithm. If the dataset-vectors are not conveniently re-arranged and set at the 3D imaging processing subroutines, the resulting image could not be acceptable. Note: at figures many times values axe-range of Kw are multiplied by  $10^{-3}$ . This type of software is developed from Author's series of previous publications in hip prostheses wear and other computational contributions [3.1, 3.6]. [Casesnoves Bioengineering Laboratory Software 2025-M-5].

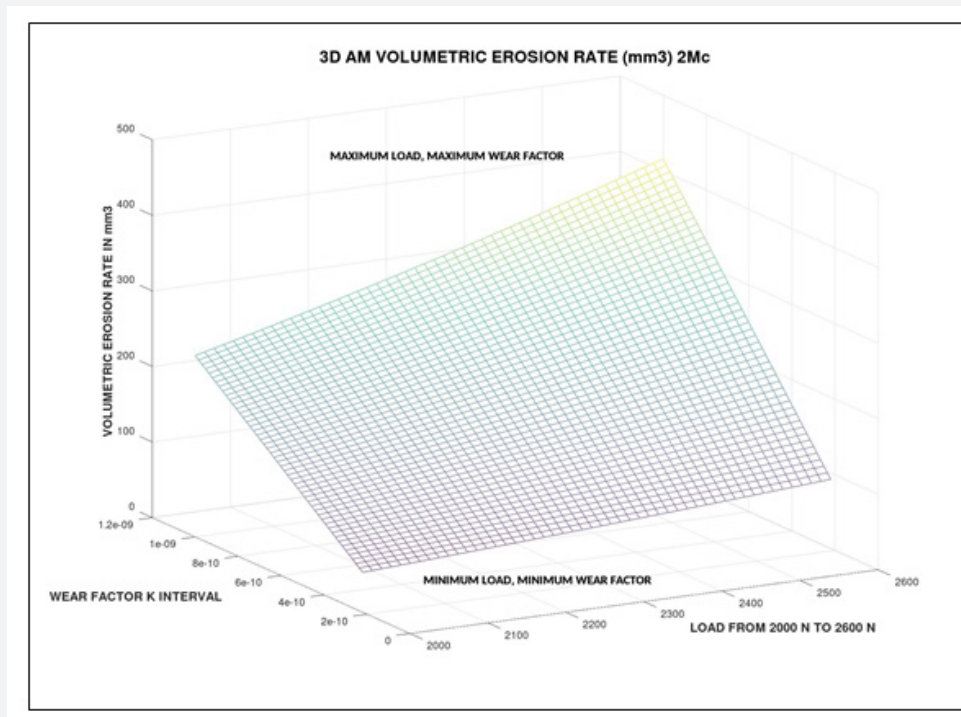


**Figure 3:** (2 Mc) GNU-Octave simulation of PE cross-shear model according to dataset of [1.1-1.4]. [Casesnoves Bioengineering Laboratory Software 2025-M-2]. These numerical magnitudes are set in Tables 1- 2. Note inset, erosion maxima and minima description.

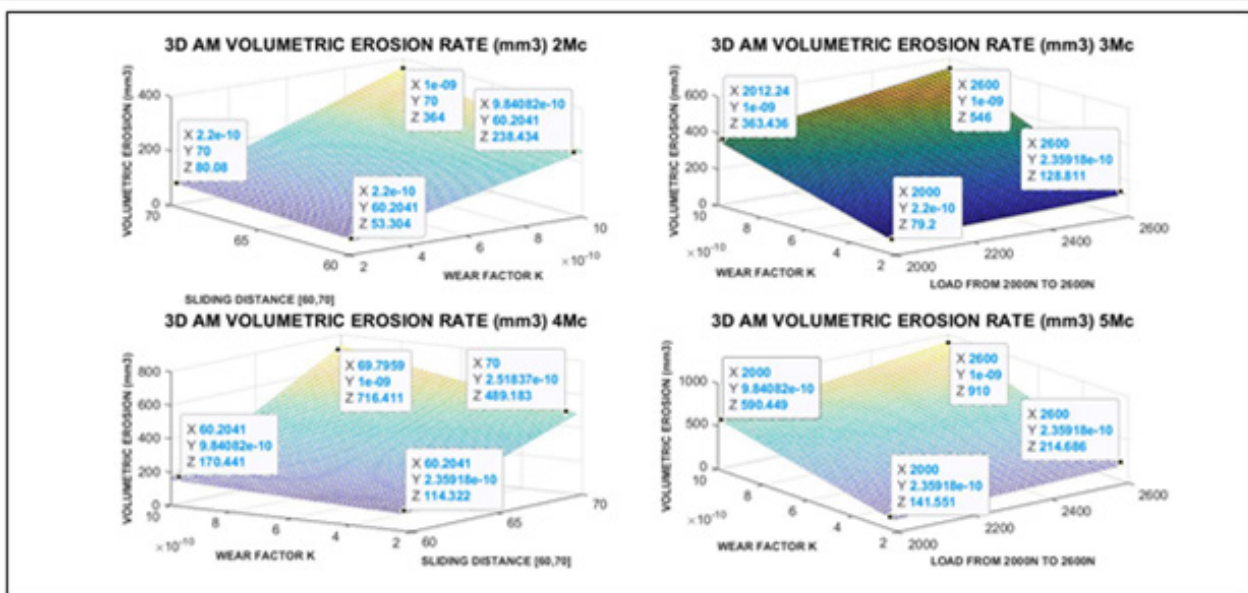


**Figure 4:** (2-5 Mc) Matlab multisimulation of PE-AM according to dataset of [1.1-1.4]. [Casesnoves Bioengineering Laboratory Software 2025-M-2]. These numerical magnitudes are set in Table 3. Numerical variations related to wear factor magnitude order create high differences in wear magnitude. It is fast/easy to extract numerical dataset from Matlab graphics.

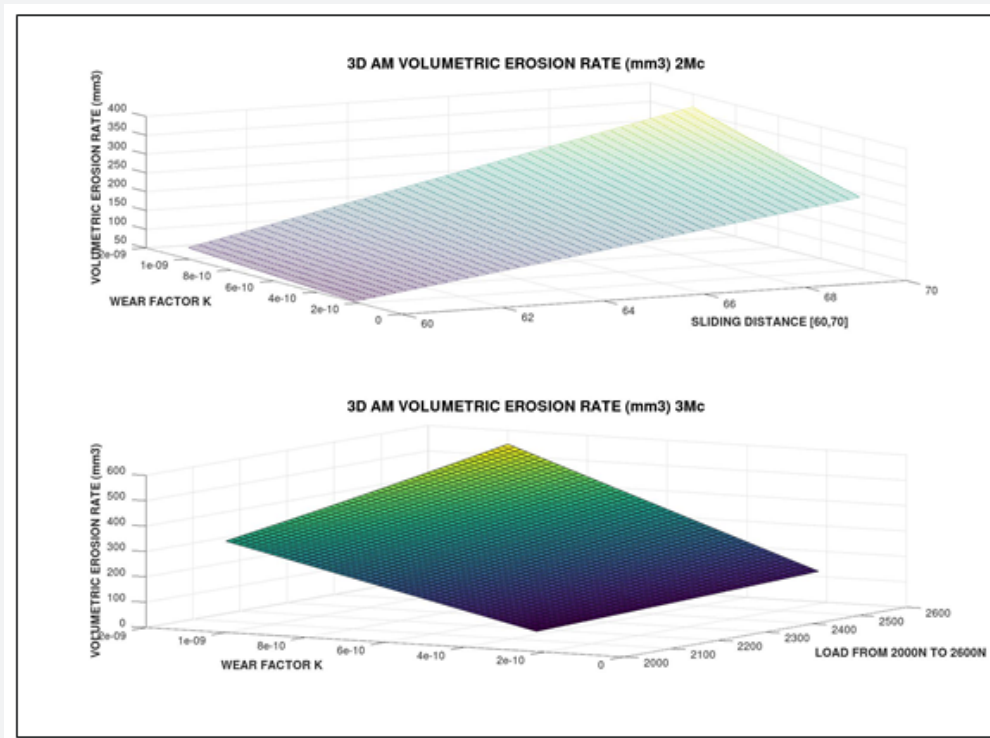


**Figure 5:** (2-3 Mc) GNU-Octave double simulation of PE-AM according to dataset of [1.1-1.4]. [Casesnoves Bioengineering Laboratory Software 2025-M-2]. These numerical magnitudes are set in Table 3.

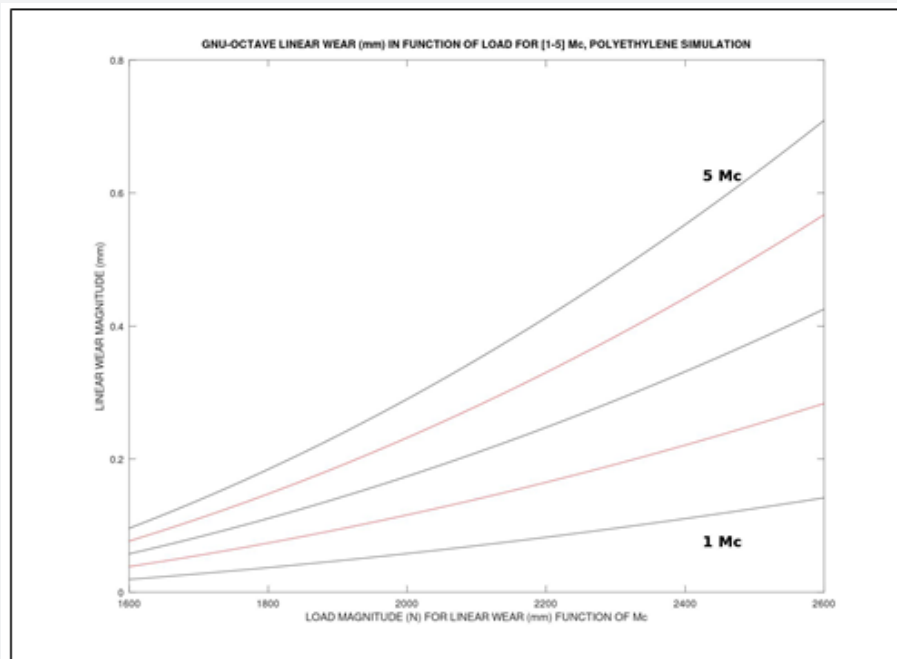


**Figure 6:** For parameters of Tables 1-2, example of polynomial fit for wear prediction in function of the load variation range of [ 1600,2600], (continuous), and Mc [1,5] (integer). It is clear the wear magnitude variation related to increase of load and the Mc number. Note: at figures values range of Kw are usually multiplied by 10<sup>-3</sup>. Previously the 2D imaging processing, a 3-degree polynomial fit was developed for every million-cycle graph-line type. This type of software is developed from Author's series of previous publications in hip prostheses wear and other computational contributions [1.5, 3.1-3.6]. [10. Casesnoves Bioengineering Laboratory Software 2025-M-3].

### Volumetric Graphical Simulations Results

Graphical results with imaging-processing are set in Figures 2.1-6. Several software designs/subroutines were used to obtain all images.

### Volumetric Numerical Results

Table 3 shows the main numerical results for AM volumetric wear with load and sliding distance intervals, extracted from Figure 4. Results are presented in max-min four intervals. Namely [60,70] mm, and [2000,2600] N. The Figure 4 cursor numerical results are used to make the Table 3.

**Table 3:** Results of Graphical Optimization and simulations for volumetric AM, [2-5] Mc, extracted from Figure 4. Software implemented dataset for simulation-optimization of volumetric AM at Tables 1-2. Wear Factor (WF) units are (mm<sup>3</sup>/ N mm). It is significant the influence of K magnitude.

AM BRIEFING NUMERICAL VOLUMETRIC RESULTS [2-5] Mc				
Mc	Erosion (mm3) for [MIN S, MIN K] (mm, WF units)	Erosion (mm3) for [MIN S, MAX K] (mm, WF units)	Erosion (mm3) for [MAX S, MIN K] (mm, WF units)	Erosion (mm3) for [MAX S, MAX K] (mm, WF units)
2	53.304	238.434	80.08	364
4	114.322	170.441	489.183	716.411
	Erosion (mm3) for [MIN L, MIN K] (N, WF units)	Erosion (mm3) for [MIN L, MAX K] (N, WF units)	Erosion (mm3) for [MAX L, MIN K] (N, WF units)	Erosion (mm3) for [MAX L, MAX K] (N, WF units)
3	79.2	363.436	128.811	546
5	141.551	590.449	214.686	910

### 8 AM Improvements-Review Linear Wear

#### Linear Wear AM Concepts-Algorithms

Primary approximations are to consider exclusively the TKA wear, and exclude Creep and Lubrication Factors, (algorithms 5-8). Therefore, the calculations of this study part constitute the improvements/review of linear wear optimization-determination to get wear durability predictions of the TKA implant with fundamental physical formulation [1.5]. In the literature, variations of models are applied, e.g. [2.1, 2.4-2.6], although the most applied is Archard’s model with several variants. Basic measurements taken into account in this study section for *in vitro* and *in vivo* and contact area correspond to [2.1-2.21]. Typical values of TKA wear, most times obtained by FE method are referred at [2.18-2.32].

#### The basic Model algorithm(s)

The basic algorithm-model from [2.3-2.11], applied and analyzed/developed mathematically by Author, reads,

*The Archard's Model applied on TKA,*

$$L_{wear} = K_{wear} \sum_{j=1}^N \left[ \sum_{i=1}^n p_i |\vec{v}_i| \Delta t_i \right]_j ;$$

[ 5. Casesnoves Bioengineering Laboratory. Algorithm-development-311]

Where,

$L_{wear}$ : Linear abrasive wear (mm).

$K_{wear}$ : Wear constant, standard (mm<sup>3</sup>/ N mm). Note: at figures values range of  $K_w$  are usually multiplied by 10<sup>-3</sup>.

$p_i$ : Pressure (N / mm<sup>2</sup>).

$v_i$ : Sliding discrete Velocity for discrete time increment (mm / s).

$\Delta t_i$ : Discrete time interval (s).

i, j: Summatory indexes. The [ i ] is for velocity variation within a cycle (n). The [ j ] is for cycles number (N).

## The Creep and Friction Factors

### Creep

Although those factors are not applied in the study, description with details of the Creep and Lubrication formulas are conveniently shown. Creep equations are usually very similar for both models, Archard's and Cross-Shear. For Creep, [2,3], the Archard's model-equation format (Lee and Pienkowski, 1998) reads,

*The Archard's Model complemented with Creep, applied on TKA,*

$$L_{total\ wear} = L_{linear\ wear} + L_{creep};$$

Hence,

$$L_{total\ wear} = L_{linear\ wear} [K_1 + K_2 (\log t-4)] P_{average} h;$$

[ 6. Casesnoves Bioengineering Laboratory. Algorithm-development-311]

where,

$K_1$ : Model Constant, [3]. Values for  $K_1$  and  $K_2$  are respectively,  $3.491 \times 10^{-3}$  and  $7.961 \times 10^{-4}$ .

$K_2$ : Model Constant, [3]. Values for  $K_1$  and  $K_2$  are respectively,  $3.491 \times 10^{-3}$  and  $7.961 \times 10^{-4}$ .

t: Time of load (minutes).

$P_{average}$ : (N/mm<sup>2</sup>)

h: Polyethylene thickness (mm)

### Friction

One common Friction Factor, set within the general formula is: [  $1+3 \mu^2$  ]<sup>1/2</sup>, [21], with values for UHMWPE of around [10<sup>-2</sup>] magnitude order. This Friction factor multiplies linearly the general formula (1). At this stage, it is not applied in the study. Friction was not set at this stage because the friction value in this case is, approximately,

$$(1+3 \times 0.072)^{0.5} = 1.0073, \text{ [ adimensional]}$$

[7. Casesnoves Bioengineering Laboratory. Algorithm-development-311]

That is, a magnitude order of 10<sup>-3</sup>. This implies that the magnitude difference if set within algorithms would not determine a magnitude order significance. That precision is useful for further refinements.

#### 1.1. The Linear Wear Integral AM Algorithm

It is convenient, when experimental data or database available, to compute the algorithm in integral-equation of first kind. Hence, taking trivial derivatives, integral, and limits for getting an integral form,

*The Archard's Model applied on TKA, integral form,*

$$L_{wear} = K_{wear} \sum_{j=1}^N \sum_{i=1}^M \left[ \int_0^{t_i} p |v| dt \right]_j ;$$

8. Casesnoves Bioengineering Laboratory. Algorithm-development-311]

where,

$L_{wear}$ : Linear abrasive wear (mm).

$K_{wear}$ : Wear constant, for programs (mm<sup>3</sup> / N mm). Note: at figures values range of  $K_w$  are usually multiplied by 10<sup>-3</sup> because of this change of units (generally  $K_{wear}$  is formulated (mm<sup>3</sup> / N x m).

p(t): Instantaneous pressure (N / mm<sup>2</sup>). Function of time.

v(t): Instantaneous sliding velocity for integral. Function of time (mm / s).

dt: Differential of time during i-interval (s).

i: Summatory index for time at every integral for a cycle (M).

j: Summatory index for total cycles (N).

*The Archard's Model on TKA, integral form proof,*

*For one cycle,*

$$L_{w1} = K_w pS;$$

Where *s* is sliding distance, hence

$$L_{w1} = K_w pvt;$$

therefore, provided  $\bar{v}$  constant and taking derivatives for time variable,

$$\frac{dL_{w1}}{dt} = K_w p\bar{v}; \text{ or;}$$

$$dL_{w1} = K_w p\bar{v}dt, \text{ integrating,}$$

$$\int_0^i dL_{w1} = K_w p\bar{v} \int_0^i dt,$$

Supposing instantaneous pressure and sliding velocity during one cycle,

Therefore, taking *N* cycles, and integrating,

$$L_{wear} = K_{wear} \sum_{j=1}^N \sum_{i=1}^M \left[ \int_0^{t_i} p |\bar{v}| dt \right]_j ;$$

[ 9. Algorithm developed by Casesnoves Bioengineering Laboratory Algorithm 3114]

### Abrasive Linear Wear Factor Kw Magnitude

Given the fact that the number of laboratory apparatus, measuring systems, and hybrid studies are profuse along the literature, there is not a total agreement for  $K_w$  magnitude [2.3]. Figures 5-6 show 2D GNU-Octave imaging processing multi-polynomial fit that describes the variation in function of  $K_w$  variation and Million Cycles [2.13-2.21] integer interval. Note: at figures values range of  $K_w$  are usually multiplied by  $10^{-3}$ . Figure 7 shows AM linear wear related to Load-Mc parameters. Figure 8 presents AM linear wear related to wear factor  $K_w$  from 1 -5 Mc. Tables 3-4.

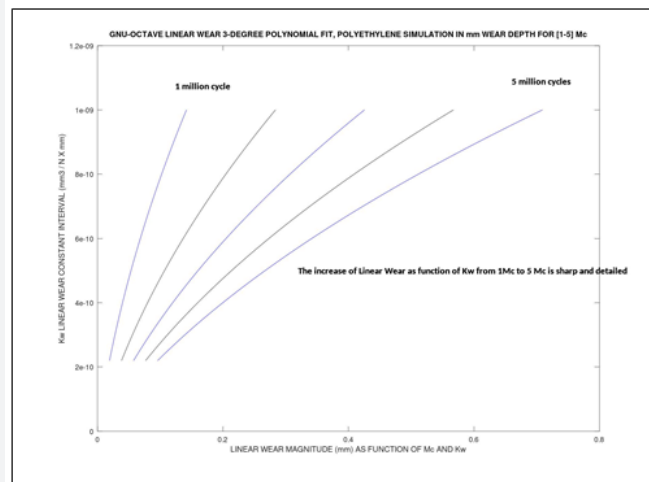


**Figure 7:** For parameters of Tables 1-2, example of polynomial fit for wear prediction in function of the variation range of [ $K_w \times 10^{-3}$ ], (continuous), and Mc [1,5] (integer). It is clear the magnitude variation related to increase of [ $K_w \times 10^{-3}$ ], and the Mc number. Note: at figures values range of  $K_w$  are usually multiplied by  $10^{-3}$ . Previously the 2D imaging processing, a 3-degree polynomial fit was developed for every million-cycle graph-line type-different from previous Figure 7. This type of software is developed from Author's series of previous publications in hip prostheses wear and other computational contributions [1.5, 3.1-3.6]. [ 11. Casesnoves Bioengineering Laboratory Software 2025-M-4].

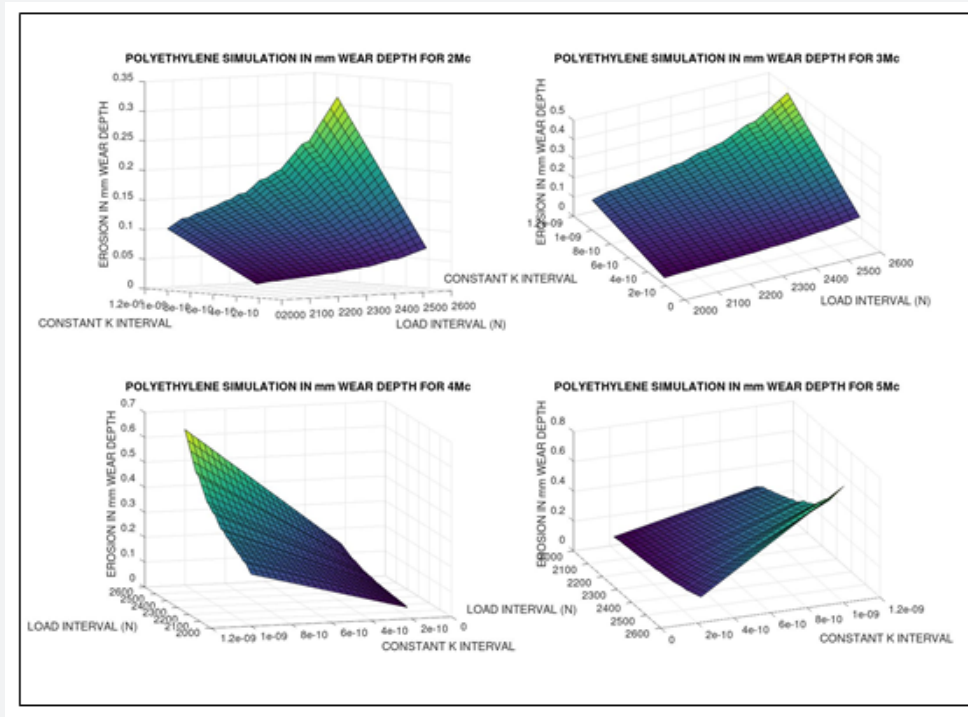


**Figure 8:** Selection of variables load and wear factor K at x-y plane. Multiple simulation with GNU-Octave for (2-5) Mc. It is shown the basic model simulated in wear mm depth (when the surface contact is implemented). It shows the different wear magnitudes when Mc are increasing. The computational method, magnitude-parameters belong to Table 3. GNU-Octave imaging-processing is acceptable. This figure software is also developed in Matlab, Figure 10. [14. Casenoves Bioengineering Laboratory Software 2025-k-3].

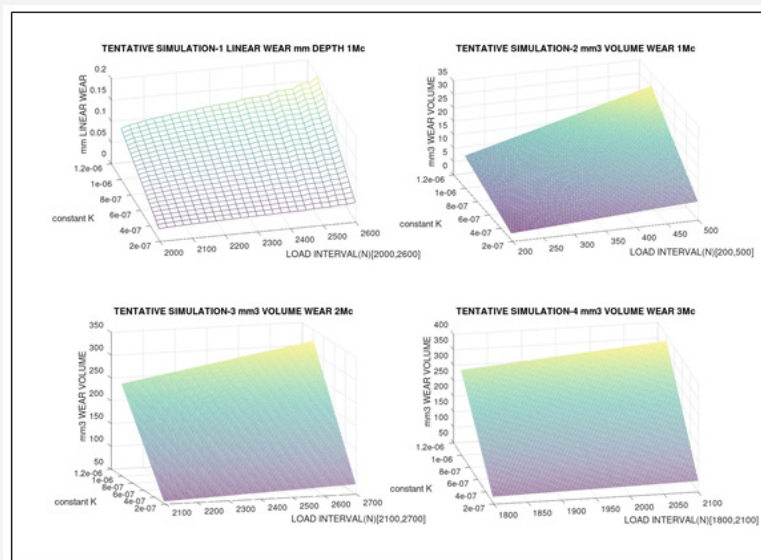


**Figure 8.1:** First trial tentative quadruple-simulation with GNU-Octave and two different 3D imaging processing subroutines (1-3) Mc. The intention is to check the different image qualities and the correct running of the programs. It is shown the basic model simulated in wear mm depth (when the surface contact is implemented), image 1, and the basic model simulated in wear mm<sup>3</sup> volume, images 1-4. Since it is tentative to show the computational method, magnitude-parameters model is not too much exact yet. However, it is clear the magnitude jumps from 10 exp (-2) to 10exp (-1) at image 1. Matlab programs are equivalent. [15. Casenoves Bioengineering Laboratory Software 2025-k-1]. The loads are varied intervals, the K wear factor constant interval is approximately [ 10<sup>-6</sup>, 10<sup>-7</sup>]. Note: at figures, not precisely here, many times values axe-range of Kw are multiplied by 10-3. [15. Casenoves Bioengineering Laboratory Software 2025-M-6]. Volumetric wear coincides with Figures 1-5.

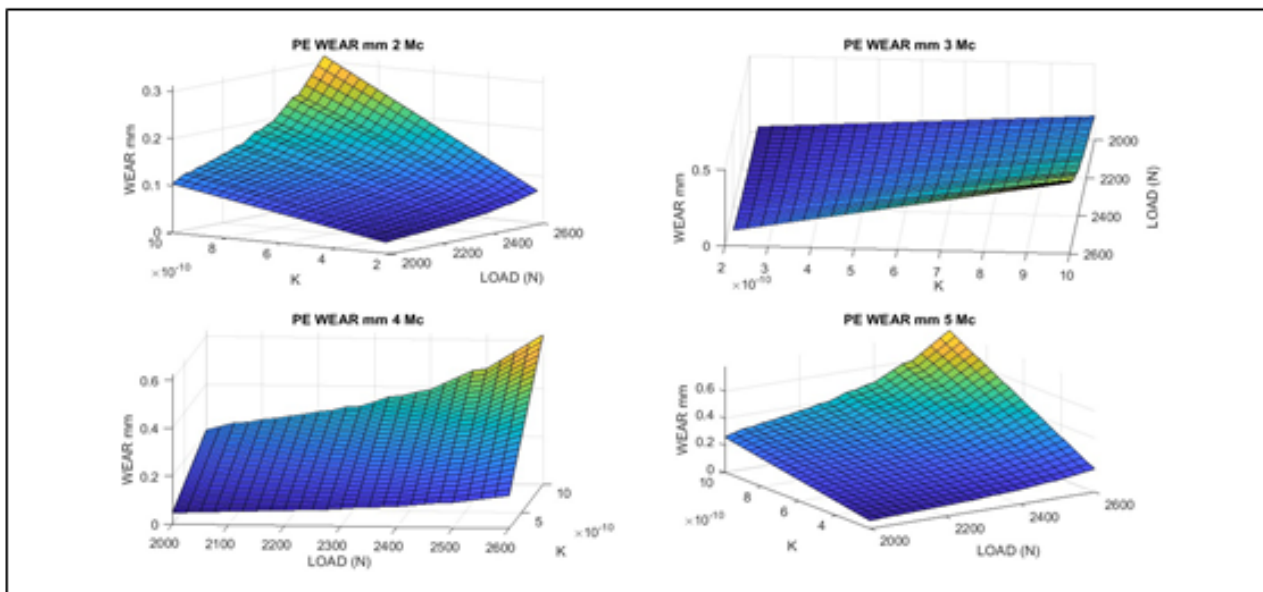


**Figure 9:** Multiple simulation with Matlab, (2-5 Mc). It is shown the basic model simulated in wear mm depth (when the surface area is implemented). It shows the different wear magnitudes when Mc are increasing. The computational method, magnitude-parameters belong to Sketchs 1-2, and Tables 4-5. Note the K wear factor constant magnitude orders. Matlab image-processing is better than GNU-Octave in this case. [16. Casesnoves Bioengineering Laboratory Software 2025-k-4].

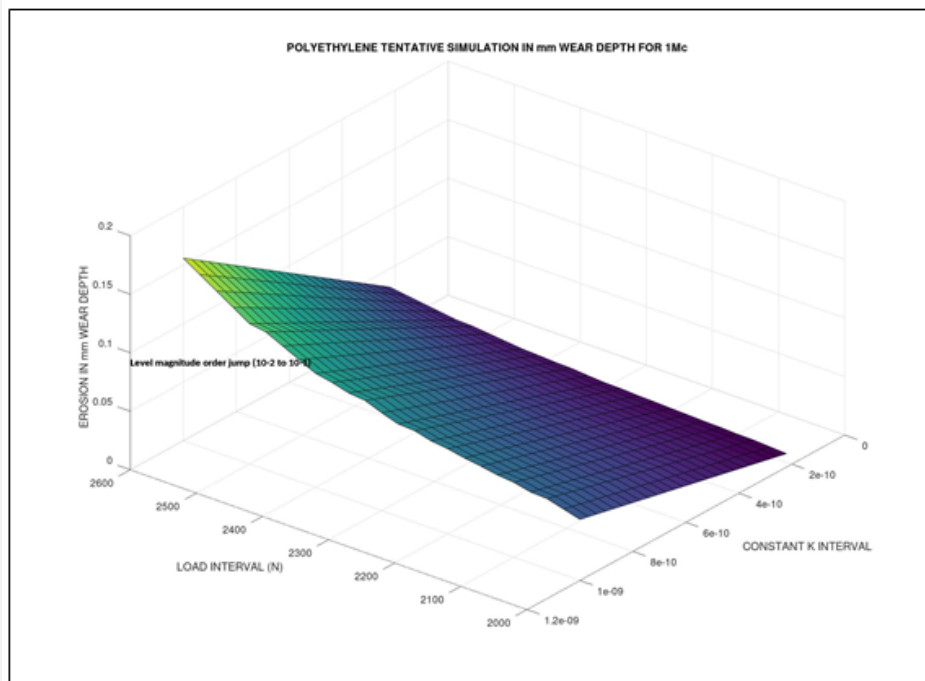


**Figure 9.1:** The purpose of this chart is to demonstrate the linear wear magnitude jump from  $10(\text{exp}-2)$  to  $10(\text{exp}-1)$ , marked inset. It is shown the basic model simulated in wear mm linear depth (when the surface contact is implemented at denominator). Matlab programs are equivalent, and in general Matlab 2D-3D image quality is superior than GNU-Octave, [17. Casesnoves Bioengineering Laboratory Software 2025-k-2]. Note: at figures many times values axe-range of Kw are multiplied by 10-3. [17. Casesnoves Bioengineering Laboratory Software 2025-M-7].

**Implemented Linear Wear Dataset and Units**

The dataset implemented for linear wear is detailed at Tables 1-2, equivalent for volumetric and linear wear data. The units for AM linear wear are included in Equation 4. The software programming was developed mainly from previous experience in hip wear models and knee articles, [1.5,3.1-3.2,3.17]. Systems used were Matlab and GNU-Octave. For programming algorithm 5, the difficulty was the matrices congruency and the loops for arrays.

**Computational intelligence Software**

The most important parts of the software are mainly two. Both are difficult. The first one is the matrices setting withing patterns and their congruence for mathematical operations. The second hurdle is the 2D-3D imaging processing subroutines setting, because not any order for getting an accurate image is efficacious when obtaining the 2D-3D image. Figure 9 Program structures, as Sketchs 1-2, were developed software programming mainly from previous experience in hip wear models [2.33-2.34]. Systems used were Matlab and GNU-Octave 8.1.0. For programming algorithms, the difficulty was the matrices congruency and the loops for arrays. Sketchs 1-2 show the software pattern to check image-processing quality, explaining the basic programming structure.

**9 AM Linear Wear Improved Results**

Results are divided into Graphical and Numerical. In this primary stage, the numerical ones were determined by Matlab graphical methods. Figure 10 The sharpness of 3D Graphical optimization is acceptable, and numerical figures show approximate coincidence with standard literature, Tables 4-5, [2.13-2.18]. Briefing of numerical comparisons to other Authors with Graphical Abstract are detailed in Table 5.

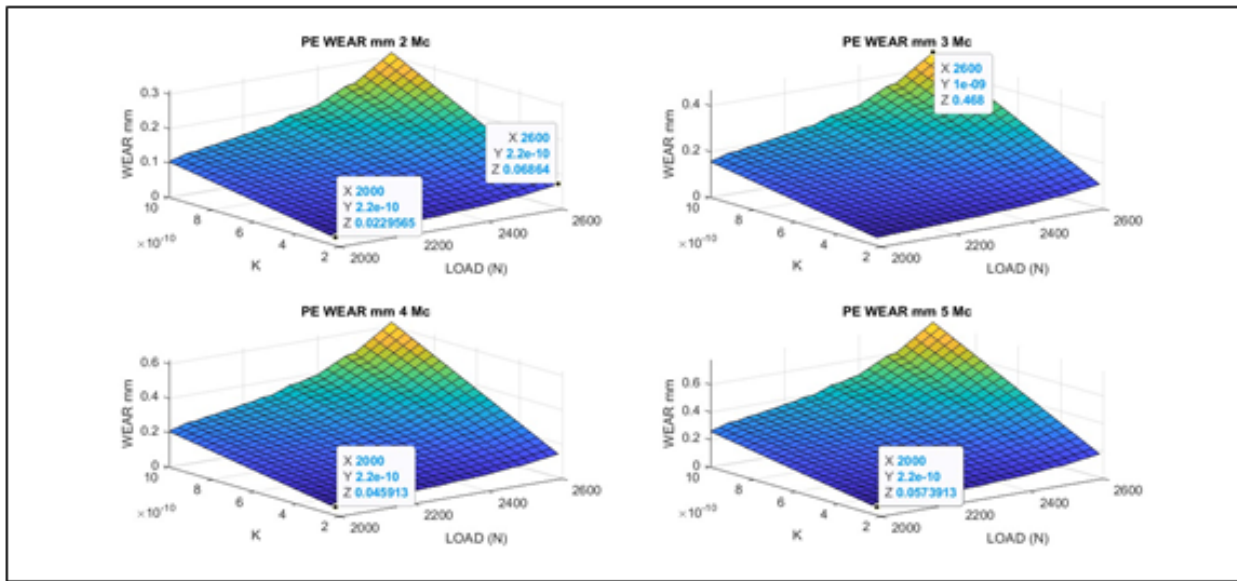


**Figure 10:** Note the cursor utility in Matlab to extract numerical data easily. A number of dataset values implemented at image. That is, a number of graphical data for multiple simulation with Matlab, (2-5 Mc). It is shown the basic model simulated in wear mm Depth (when the surface area is implemented). It proves the different wear magnitudes when Mc are increasing. Matlab image-processing is better than GNU-Octave in this case. [18. Casesnoves Bioengineering Laboratory Software 2025-k-5].

**Graphical Optimization Results**

Graphical Optimization Method was developed during PhD Thesis and PhD Program publications, later in series of articles [1.5,3.1-3.2,3.17-3.28]. It essentially consists in finding the global/local minima by searching along the implemented 2D-3D imaging surfaces/curves of the algorithm objective function plus one/two selected parameters. Figure 11 Here it is applied on the wear formulas (3,6,8) to determine the optimal minima or any desired values subject

to particular constraints along the 3D surface. In Illustrative Example 1, it can be seen the process initiation. Firstly, some tentative programs are designed, after that, when checking the functionality of the software and the numerical congruence of the 3D graphs, the definite 3D Graphical Optimization Image-Processing charts are done with accurate parameters and intervals (Figure 12-14.1).

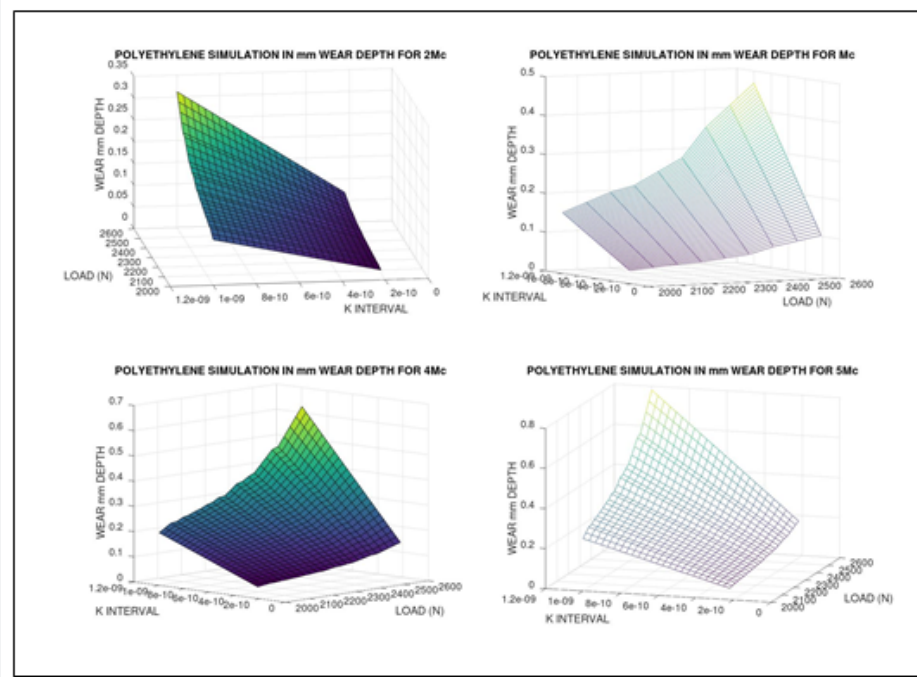


**Figure 10.1:** Multiple simulation, by using the program of Figure 9, but modified. Two different 3D imaging processing subroutines, with GNU-Octave for (2-5) Mc. It is shown the basic model simulated in mm depth wear (when the surface contact is implemented). It shows the different wear magnitudes when Mc are increasing. The computational method, magnitude-parameters belong to Tables 1-2. GNU-Octave imaging-processing is acceptable. This figure software is also developed in Matlab, Figures 10-11. [19. Casesnoves Bioengineering Laboratory Software 2025-k-3]. Note: at figures many times values axe-range of Kw are multiplied by 10-3. This type of software is developed from Author's series of previous publications in hip prostheses wear and other computational contributions [3.1-3.6,3.28].

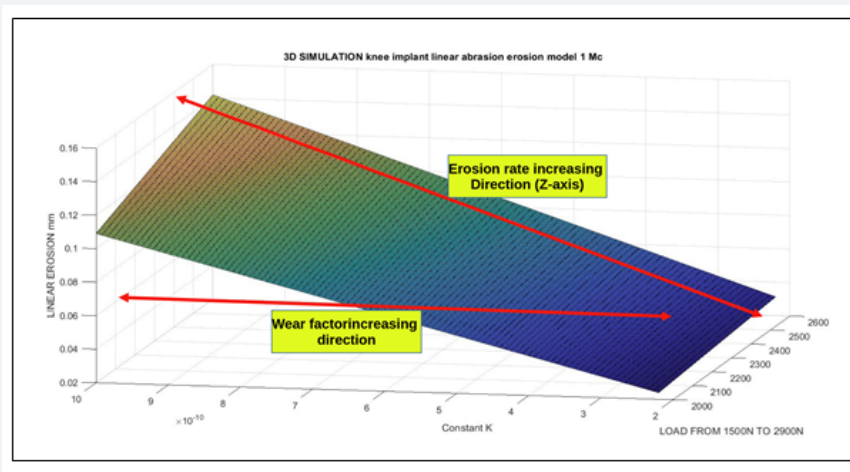


**Figure 11:** Matlab demonstration with graphical simulation for magnitude changes. It is done with a different/simpler program for 1 Mc. It is shown the basic AM model simulated in wear mm depth. It shows the different wear magnitudes when loads are increasing. [20. Casesnoves Bioengineering Laboratory Software 2025-k-6].

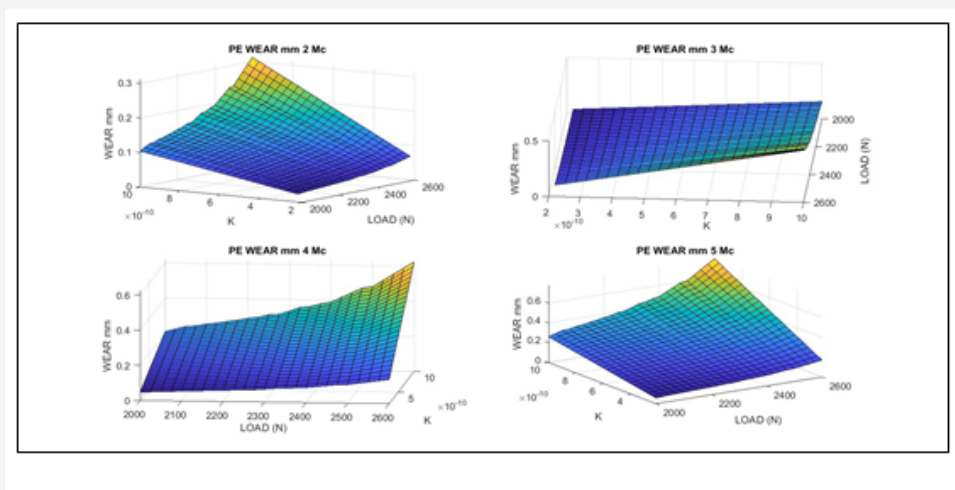


**Figure 11.1:** Numerical details in multisimulation with Matlab, (2-5 Mc). It is shown the basic model simulated in wear mm depth (when the surface area is implemented). It shows the different wear magnitudes when Mc are increasing. The computational method, magnitude-parameters belong to Tables 1-2, and method to Sketchs 1-2. Note the wear factor K constant magnitude orders. Matlab image-processing is better than GNU-Octave in this case. [21. Casesnoves Bioengineering Laboratory Software 2025-M-9].

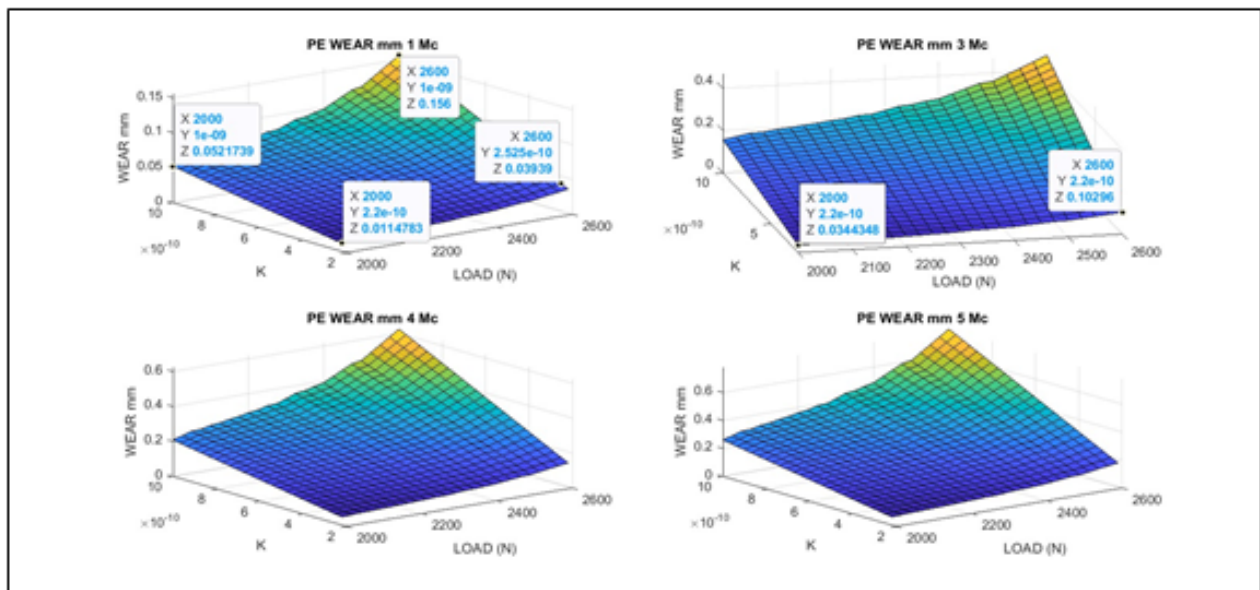


**Figure 12:** Matlab multisimulation for catching up the differences among 1 Mc and 3,4,5 Mc, it is shown a number of graphical data for multiple simulation with Matlab (dataset of 1,3 Mc included). Image-processing displays the different wear magnitudes when Mc are increasing. Matlab has several 3D imaging processing tools. Matlab image-processing is better than GNU-Octave in this case. [ 22. Casesnoves Bioengineering Laboratory Software 2025-k-7].

**AM Linear Wear Numerical Results**

Graphical Abstract within (Table 5) and tabulated magnitudes show extracted from Graphical Optimization the numerical data results for linear wear. Figures and magnitude orders match the standard literature. Those magnitude values can be compared at [2.1-2.32] further

references.

**Comparison of Numerical Results**

Graphical abstract within (Table 5) presents some numerical comparisons with other literature studies. Some of them are carried out with FE Method, others with FE

Method and contrasted with cadaveric data. The most important objective consequence is that from [2,3] Mc on, the Linear Erosion shows a magnitude order jump from  $10^{-2}$  to  $10^{-1}$  mm. The comparisons are shown for database from [2.13-2.17]. However extensive further database can be found at [2.18-2.32] (Table 6).

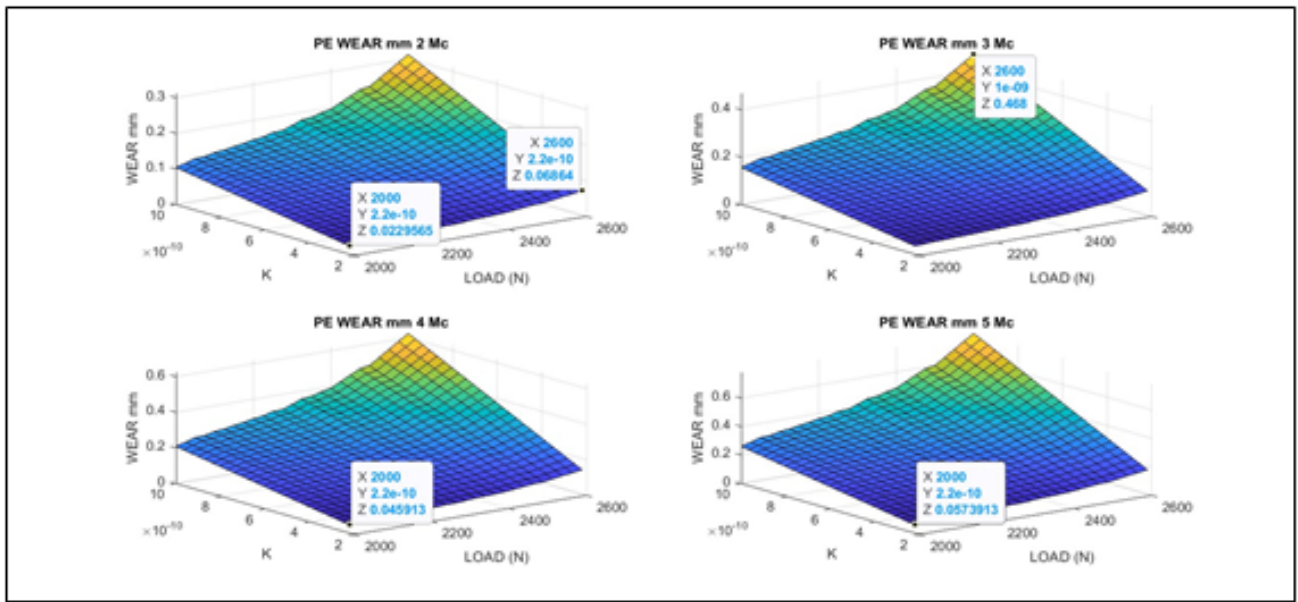


**Figure 12.1:** From previous Figures, a number of dataset values implemented at image. That is, a number of graphical data for multiple simulation with Matlab, (2-5 Mc), magnitude values inset. It is shown the basic model simulated in wear mm Depth (when the surface area is implemented). [23. Casenoves Bioengineering Laboratory Software 2025-k-5].

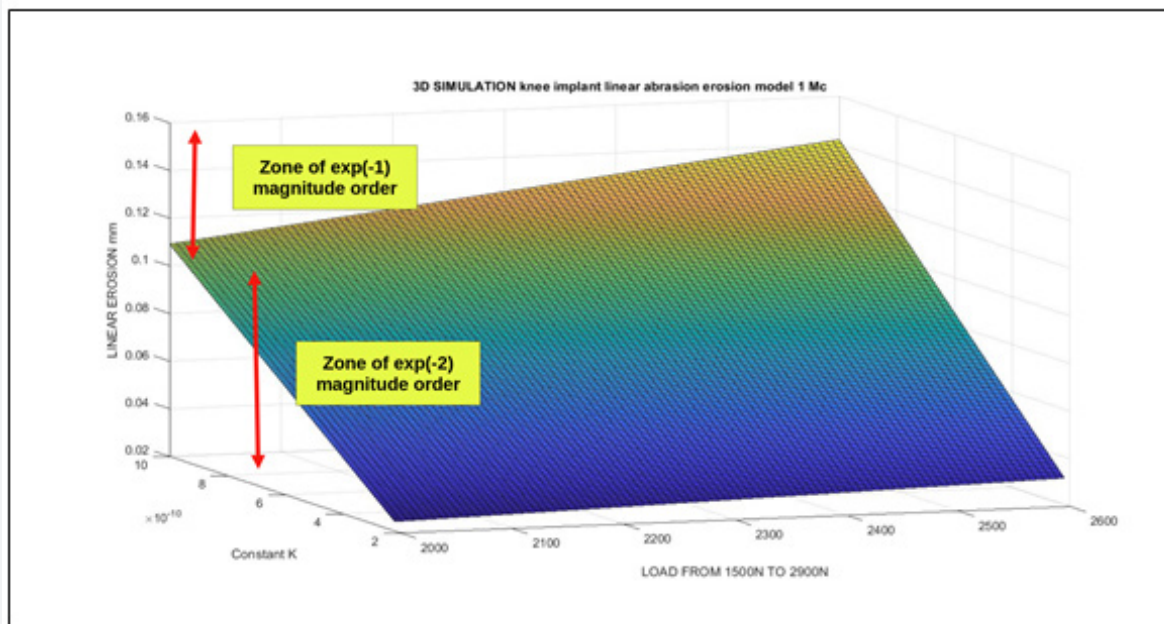


**Figure 13:** A different perspective for software of Figures 12. Matlab graphical simulation with a simpler program for 1 Mc. It is shown the basic model simulated in wear mm Depth. It is clear the different wear magnitudes when loads are increasing. [24. Casenoves Bioengineering Laboratory Software 2025-k-8].

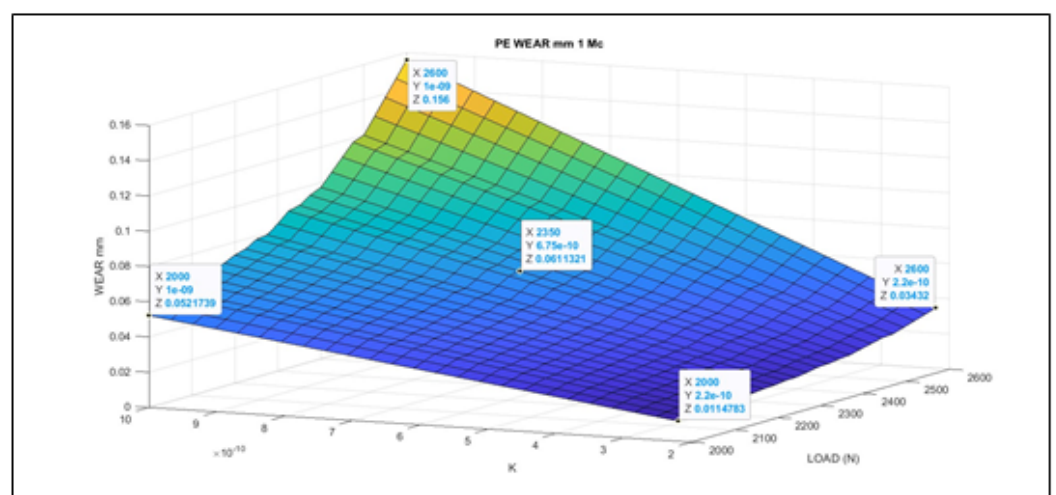


**Figure 14:** Setting the display of dataset for Figures 12. Matlab program is simple. The dataset inset is used for Tables 4-5 of results. [ 25. Casenoves Bioengineering Laboratory Software 2025-k-9].

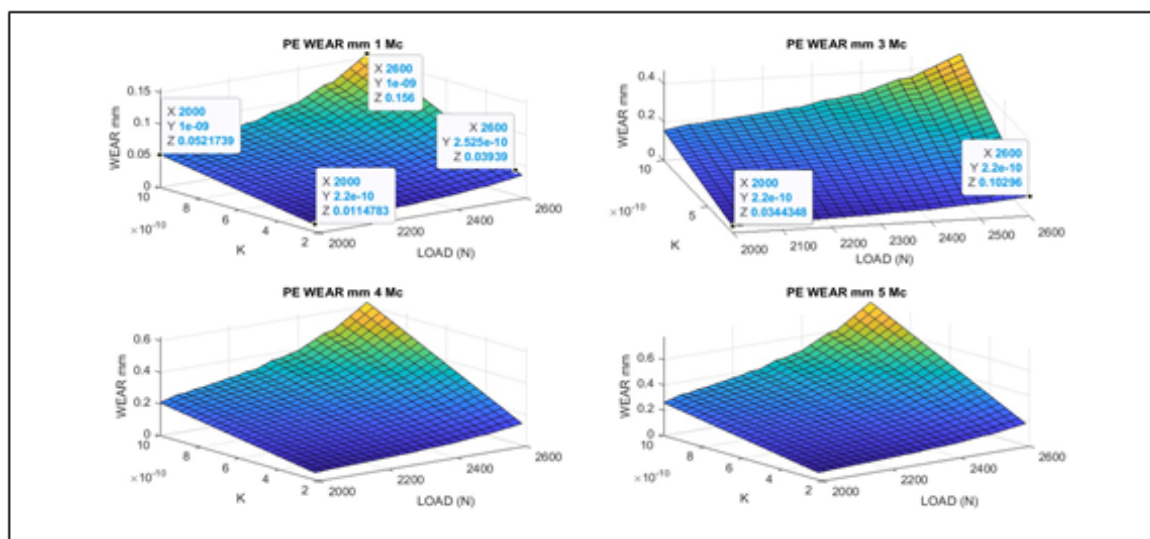


**Figure 14.1:** For catching up maxima and minima differences among 1 Mc and 3,4,5 Mc, it is shown a number of graphical data for multiple simulation with Matlab (dataset of 1,3 Mc included). Image-processing displays the different wear magnitudes when Mc are increasing. [ 26. Casenoves Bioengineering Laboratory Software 2025-k-7].

### Discussion and Conclusion

The objectives of the research were two. First, to develop AM volumetric wear integer and integral equations. Secondly, simulate/compare the PE volumetric wear without creep AM predictions for TKA in a primary approximation. Complementary, an AM linear wear

improvements from previous publications were included. Graphical Optimization for AM, numerical results, and comparison with literature dataset were presented. Some programming-recipes to develop simulation-software and an applications briefing were included. At this stage, Lubrication Factors for the models were not set.

**Table 4:** Graphical abstract and main numerical results in the study. Magnitudes match standard literature, [2.1-2.32], Those magnitude values can be compared at [2.1-2.32] further references.

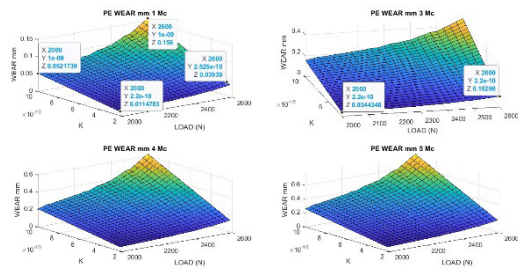
AM LINEAR WEAR NUMERICAL RESULTS						
				<p>The Archard's Model on TKA, integral form proof, For one cycle, <math>L_{w1} = K_w pS;</math> Where <math>S</math> is sliding distance, hence <math>L_{w1} = K_w pv;</math> therefore, provided <math>\bar{v}</math> constant and taking derivatives for time variable, <math>\frac{dL_{w1}}{dt} = K_w p;</math> or; <math>dL_{w1} = K_w pvd;</math> integrating, <math>\int dL_{w1} = K_w \int pvd;</math> Supposing instantaneous pressure and sliding velocity during one cycle, Therefore, taking <math>N</math> cycles, and integrating, <math display="block">L_{wear} = K_{wear} \sum_{j=1}^N \sum_{i=1}^M \left[ \int_0^i p  v  dt \right]_j ;</math></p>		
Mc	AM RESULTS MINIMA			AM RESULTS MAXIMA		
	WEAR (mm)	WEAR COEFFICIENT KW (mm <sup>3</sup> / (N x mm))	LOAD (N)	WEAR (mm)	WEAR COEFFICIENT KW (mm <sup>3</sup> / (N x mm))	LOAD (N)
1 Mc	0.01	2.2 x 10 <sup>-10</sup>	2000	0.16	10 <sup>-9</sup>	2600
2 Mc	0.02	2.2 x 10 <sup>-10</sup>	2000	0.31	10 <sup>-9</sup>	2600
3 Mc	0.03	2.2 x 10 <sup>-10</sup>	2000	0.46	10 <sup>-9</sup>	2600
4 Mc	0.05	2.2 x 10 <sup>-10</sup>	2000	0.62	10 <sup>-9</sup>	2600
5 Mc	0.06	2.2 x 10 <sup>-10</sup>	2000	0.78	10 <sup>-9</sup>	2600
PRECISION	The mathematical distribution is almost linear for the wear magnitudes.			The mathematical distribution is less linear.		

Volumetric wear rates are primary results in this research, to be improved in next studies. The graphs obtained are acceptable and abrasive volumetric wear numerical results match approximately the standard dataset published, Figures 2.1-5, (Table 3). According to Table 3, the variation of volumetric wear related to wear factor is high. The higher wear factor, the higher volumetric rate variation in approximately exponential curves, Figure 2, Table 3. The calculated dataset at Table 3, from graphical optimization matches the published literature mostly [1.1-1.12]. Provided the wear factor value can be selected from graphics intervals Table 3, numerical dataset coincides approximately with other authors publications [1.1-1.12]. The load shows be also a significant magnitude parameter for prediction calculations-at least one magnitude order. The higher load, the higher volumetric wear rate, Figures 2, 2.1-5, Table 3. Roughly speaking, the volumetric wear can be approximated from the linear wear multiplied by the magnitude order of contact area, Equations 1-3. This approach confirms the results of this study.

**Table 5:** Table with Graphical Abstract of AM comparative numerical results. The wear magnitudes and rates differ in literature and laboratories for

two main reasons: (1) the large variety of testing apparatus and methods, and the ISO variants also, (2) the large variety to communicate/measure results. Namely, wear per Mc (mm), wear per year (mm), wear per Mc (mg), wear per year (mg), and others. When the study is *in vivo*, wear is usually expressed in mm/year, because the *in vivo* testing takes the sample data usually from patients or recent cadaveric samples whose medical histories show the date when the arthroplasty was done. What is common in all literature, is the polyethylene density approximately equal to water. Magnitude orders match standard literature, [2.3,2.11,2.13-2.18]. Additional complementary dataset can be found at [2.19-2.32]. FE method is used in general for both comparisons/validations with *in vivo* measurements. Computational Optimization and general Bio tribology concepts can be read at [8.33-8.36]. comparisons with other literature studies. Results match in magnitude order these authors dataset.

ARCHARD MODEL COMPARATIVE NUMERICAL RESULTS TO LITERATURE



RESULTS APPROXIMATED FOR ALL COMPARISONS CALCULATIONS, WHEN IN VIVO, IT IS TAKEN FROM [2.16], AN AVERAGE OF 2Mc BY YEAR

Mc [AP-PROX]	AUTHOR'S STUDY LINEAR WEAR (mm)	1 [2.13, wear+creep,2002] [in vivo, 69 patients, geometrical extrapolation from graphics]	2 [2.14,2019] [in vivo, 49 patients] This author shows dataset for maximum wear, lateral (Lat), and medial (Med). It is shown [ref], Lat= [0.034,0.069]/year, and Med+ [0.04,0.069]. All angles. LAT: lateral implant zone MED: medial implant zone	3 [2.15, wear+creep,2019] [in vivo, 106 patients] This Author shows 0.015 mm/year (supine), and 0.220 mm/year (standing). Proportional Average set by this study Author, is calculated here as, (4 x standing supine) / 5 = 0.1790. Approx=0.18/year.	4 [2.17, 2022] [in vivo-in-vitro, FE compared to 1 cadaveric sample, Flex+ AP, geometrical extrapolation from graphics]
1 Mc	[0.01,0.16]	[0.001,0.01]	LAT [0.02, 0.03] MED [0.02,0.03]	[0.09]	[0.03]
2 Mc	[0.02,0.31]	[0.01,0.20]	LAT [0.03,0.07] MED [0.04,0.07]	[0.18]	[0.08]
3 Mc	[0.03,0.46]	[0.50,1.00]	LAT [0.07,0.09] MED [0.06,0.09]	[0.27]	[0.09]
4 Mc	[0.05,0.62]	[1.00,1.10]	LAT [0.08,0.12] MED [0.08,0.12]	[0.36]	[0.10]
5 Mc	[0.06,0.78]	[1.10,1.20]	LAT [0.10,0.15] MED [0.10,0.15]	[0.45]	[0.13]
COMMENTS	Almost linear the wear magnitudes when Mc number is low, proportional to Mc number. Differences tend to get nonlinear in function of Mc, when the Mc magnitude increases.				
IMPORTANT PRECISION	THE WEAR MAGNITUDES AND RATES DIFFER IN LITERATURE AND LABORATORIES FOR TWO MAIN REASONS: (1) THE LARGE VARIETY OF TESTING APPARATUS AND METHODS, (2) THE LARGE VARIETY TO COMMUNICATE/MEASURE RESULTS. NAMELY, WEAR PER Mc (mm), WEAR PER YEAR (mm), WEAR PER Mc (mg), WEAR PER YEAR (mg), AND OTHERS. WHEN THE STUDY IS IN VIVO, WEAR IS USUALLY EXPRESSED IN mm/YEAR. WHAT IS COMMON IS THE POLYETHYLENE DENSITY APPROXIMATELY EQUAL TO WATER [2.13-2.18]. ADDITIONAL COMPLEMENTARY DATASET CAN BE FOUND AT [2.18-2.32].				

**Table 6:** Biomechanical and Bio Tribological applications briefing. Some of them are similar to previous studies in hip joint wear [3.1-3.2]. Further reading and laboratory techniques/applications can be found at [1.1-1.7, 2.1-2.32].

TKA BIOTRIBOLOGY I+D AND BIOMECHANICS-CLINICAL APPLICATIONS	
<b>MANUFACTURING MAIN UTILITY IN COMPUTATIONAL BIOENGINEERING</b>	TKA Wear Predictions and efficacious calculations at 3D image-processing graphs, especially with Matlab, to know the exact magnitude for any selected Wear Coefficient (AM), or Wear Factor (CSM model) constants and Load (x, y, coordinates), the approximate predictions of abrasive wear magnitude for 1-5 Mc.
<b>TOTAL WEAR AND BIOTRIBOLOGY BIOMATERIAL PREDICTIONS</b>	For specific UHMWPE material types design/manufacturing of TKA prostheses. TKA erosion prediction, especially for polyethylene materials, is essential, since this polymer is the most widely used in TKA, [2.1-2.32]. Prediction saves manufacturing-research time, repeating laboratory work, and budget.
<b>TKA AVERAGE-DURABILITY PATIENT PREDICTION</b>	Any patient is subject and informed about the lifetime of the TKA implant surgically set. To provide patient with quality of life during implant functional time. What is more, to avoid re-operations and substitution with new prostheses.
<b>BIOMEDICAL INDUSTRIAL MANUFACTURING</b>	The biomedical manufacturing methods are continuously improving. In this line, optimization of manufacturing process and quality improvement is required.
<b>I+D RESEARCH AND CLINICAL RESEARCH</b>	The TKA prostheses are in continuous evolution. For future design of new types. Similar/variants of materials I+D.
<b>PATIENT LIFE QUALITY</b>	Very important for normal movement of patient. Walk and essential movements easy and comfortable for any patient during all duration time.
<b>SPORT MEDICINE ADVANCES</b>	The sport medicine constraint is tougher than common patient conditions. From the average patient knowledge/investigation, progress for sport medicine TKA implants can be got. This is a very important application because sport-medicine requires these prostheses with higher quality than usual patients.

For 1 Mc AM abrasive linear wear is of the magnitude order [  $10^{-2}$ ,  $10^{-1}$  ], and these predictions are more exact than primary volumetric findings. For Cross-Shear Type Models (CSM), [1.1-1.3], not included in this study, but software-calculated, the linear wear magnitude is higher, around  $10 \exp(-1)$  for 1 Mc. At linear AM in 1 Mc. at second review-part, the proven magnitude jump for this linear AM wear is presented as much clearly as possible, for instance, (Illustrative Examples 1-2).

It is significant, the rather strong influence of Wear Factor (WF) K in volumetric magnitude results, Table 3. WF magnitude varies according to authors actually, [2.3]. Numerical and graphical optimization results for AM volumetric wear match approximately the published ones. Advantages of this method related to FE technique are the fast results, and graphical visualization/comparison of results. Inconveniences are the software precision/equations developments that have to be checked. Another inconvenient is the matrices congruence arrange along program-patterns, both Matlab and GNU-Octave systems [3.29-3.45].

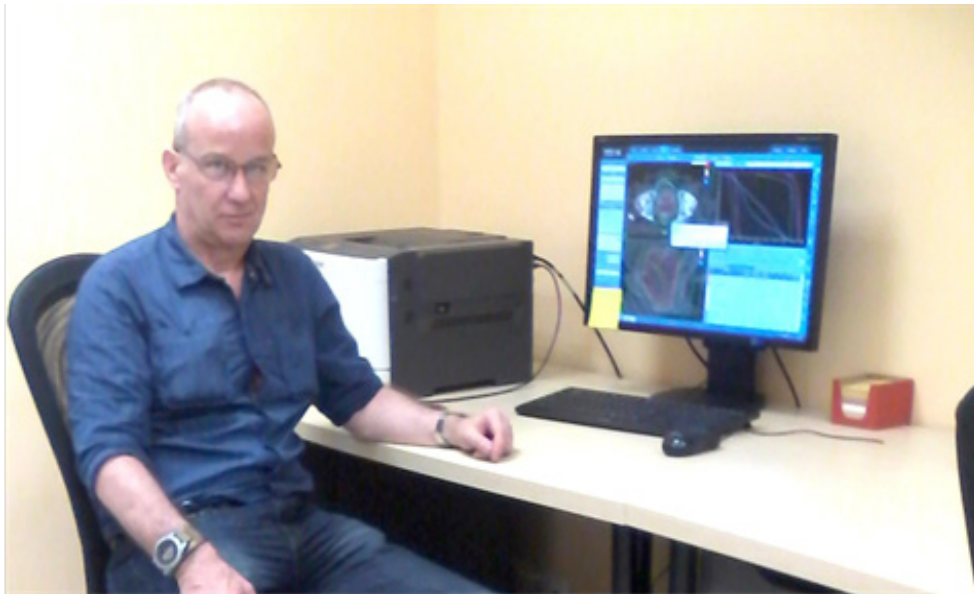
The image processing quality in GNU-Octave and Matlab is acceptable. It was tried to approximate/approach the most common numerical and graphical results published, given the large variety of variants for mathematical models-methods and ISO norms for TKA volumetric wear implants predictions.

In brief, a primary Graphical Simulations-Optimizations series for PE TKA implants abrasive volumetric erosion with AM were presented. Results for AM volumetric wear match approximately the literature figures and standards. Applications in Biotribology and Mathematical Optimization-Simulations are presented.

### Scientific Ethics Standards

According to European Union and International Scientific Ethics [3.46-3.48]. All the software was done by Author. No Artificial Intelligence (AI) used for programming or any article-part, if wear so, it is declared, both in tools/systems for software anyway, and AI browsers-information. When any mathematical statement, algorithm/proposition/theorem is presented, demonstration and parameters/units are always detailed. Review of linear wear, algorithms and images, is selected from previous publications. If any inconsistency is found after publication, it is clarified in subsequent ones. When a citation such as [ Casesnoves, 'year' ] is set, it is to clarify intellectual property at current times, without intention to brag. The article is exclusively scientific, without commercial, institutional, academic, deliberate obfuscation, religious or religious influences, non-scientific theories, personal opinions, political ideas, or economical-conflict links. Author has no conflict of interest.

### Author's Biography



Dr Francisco Casesnoves earned the Engineering and Natural Sciences PhD by Tallinn University of Technology (started thesis in 2016, thesis Defence/PhD earned in December 2018, official graduate Diploma 2019). Dr Casesnoves is European Union and Internationally qualified as Doctor in Engineering to supervise PhD Theses, Master Theses, and Bachelor Theses in science and engineering. He works as independent research scientist in computational-engineering/physics. Dr Casesnoves earned MSc-BSc, Physics/Applied-Mathematics (Public Eastern-Finland-University, MSc Thesis in Radiotherapy Treatment Planning Optimization, which was developed after graduation in a series of Radiation Therapy Optimization-Modelling publications [2007-present]). Dr Casesnoves earned Graduate-with-MPhil, in Medicine and Surgery [1983] (Madrid University Medicine School, MPhil in Radioprotection Low Energies Dosimetry [1985]). He studied always in public-educational institutions, was football player 1972-78 (defender and midfielder) and as Physician, supports healthy life and all sports activities. Casesnoves resigned definitely to his original nationality in 2020 for ideological reasons, democratic-republican ideology, ethical-professional reasons, anti-state monarchy corruption positions, and does not belong to Spain Kingdom anymore. His constant service to the International Scientific Community and Estonian technological progress (2016-present) commenced in 1985 with publications in Medical Physics, with further specialization in optimization methods in 1997 at Finland-at the moment approximately 100 recognized publications with approximately 65 DOI papers. His main branch is Computational-mathematical Nonlinear/Inverse Methods Optimization. Casesnoves best-achievements are the Numerical Reuleaux Method in dynamics and nonlinear-optimization [books 2019-2020], The series of Radiotherapy Improvements for AAA superposition-convolution model, the Graphical and Interior Optimization Methods [2016-8], the new Computational Dissection-Anatomical Method, [2020], invention of Forensic Robotics [2020-2021], invention of 3D Isodoses in radiotherapy TPO, and Molecular Effect Model for High Temperature Superconductors [2020]. Dr Casesnoves PhD thesis is an Estonian scientific service to European Social Fund and several EU Research Projects. Dr Casesnoves scientific service since 2016 to the Free and Independent Republic of Estonia for technological development (and also at Riga technical University, Power Electrical and Electronics Department) is about 40 physics-engineering articles, two books' series, and 1 industrial radiotherapy project associated to Europe Union EIT Health Program (Tartu University, 2017).

## References

### 1. Numeration-References TKA Specific for Volumetric and Linear Wear

- 1.1. Abdelgaied A, Colls (2010) Computational wear prediction of artificial knee joints based on a new wear law and formulation. *Journal of Biomechanics* 44 (6): 1108-1116.
- 1.2. Kang I, et al. (2008) Quantification of the effect of cross-shear on the wear of conventional and highly cross-linked UHMWPE. *Journal of Biomechanics* 41 (2): 340-346.
- 1.3. Abdelgaied A, Colls (2018) A comprehensive combined experimental and computational framework for pre-clinical wear simulation of total knee replacements. *Journal of the Mechanical Behavior of Biomedical Materials* 78 (2018): 282-291.
- 1.4. Shiramizu K, Colls (2009) Tibiofemoral contact areas and pressures in six high flexion knees. *International Orthopaedics (SICOT)* 33: 403-406.
- 1.5. Casenoves F (2025) Computational simulations-optimization of UHMWPE knee arthroplasty abrasive wear, Second Part. *International Journal of Basic and Applied Medical Sciences* 2.
- 1.6. Abdelgaied A, Colls (2022) Understanding the differences in wear testing method standards for total knee replacement. *Journal of the mechanical behavior of biomedical materials* 132: 105258.
- 1.7. Haider H, Garvin K (2008) Rotating Platform versus Fixed-bearing Total Knees. *Clin Orthop Relat Res* 466: 2677-2685.
- 1.8. Teeter M, Colls (2015) Wear and Creep Behavior of Total Knee Implants Undergoing Wear Testing. *The Journal of Arthroplasty* 30(1): 130-134.
- 1.9. Fekete G, Colls (2022) Wear Modelling of Total Knee Replacements. *Acta Materialia Transylvanica* 5/2: 66-71.
- 1.10. Goodman S, Lidgren L (1992) Polyethylene wear in knee arthroplasty. *Acta Orthor, Scand* 63(3): 358-364.
- 1.11. Darmanto D, Colls (2026) Wear Performance Analysis of UHMWPE for Total Knee Arthroplasty. *Engineering, Technology & Applied Science Research* 16(1): 31393-31400.
- 1.12. Kayaro CE, Colls (2024) Early monitoring of inlay wear after total knee arthroplasty on plain radiographs using model-based wear measurement. *Scientific Reports* 14: 18248.

### 2. Numeration-References TKA General

- 2.1. Dawim P (2013) *Biomaterials and medical tribology. Research and development.* Woodhead Publishing.
- 2.2. Schaldach M, Hohmann D (1976) *Advances in artificial hip and knee joint technology.* Springer.
- 2.3. Jin Z (2014) *Computational Modelling of Biomechanics and Biotribology in the Musculoskeletal System.* Woodhead Publishing.
- 2.4. Munzinger U, Boldt J, Keblish P (2004) *Primary knee arthroplasty.* Springer.
- 2.5. Dawim P (2010) *Biotribology.* Wiley.
- 2.6. Sculco T, Martucci E (2001) *Knee Arthroplasty.* Springer.
- 2.7. Emre TE, Colls (2023) *Total Knee Arthroplasty. A Review of Medical and Biomedical Engineering and Science Concepts.* Springer.
- 2.8. Kumar A, Colls (2024) *Applications of Biotribology in Biomedical Systems.* Springer.
- 2.9. Kretzer J (2014) Wear in total knee arthroplasty-just a question of polyethylene? *International Orthopaedics (SICOT)* 38: 335-340.
- 2.10. D'Lima D (2007) *Doctoral Thesis. In vivo tibial force measurement after total knee arthroplasty.* UC San Diego Electronic Theses and Dissertations.
- 2.11. Affatato S (2012) *Wear of orthopaedic implants and artificial joints.* Woodhead Publishing Limited.
- 2.12. Triwardono J, Colls (2021) Evaluation of the Contact Area in Total Knee Arthroplasty Designed for Deep Knee Flexion. *International Journal of Technology* 12(6): 1312-1322.
- 2.13. Hoshino A, Colls (2002) Accurate in vivo measurement of polyethylene wear in Total Knee Arthroplasty. *The journal of Arthroplasty* 17(4).
- 2.14. Teeter M, Colls (2019) Radiostereometric analysis permits in vivo measurement of very small levels of wear in TKA. *Clin Orthop Relat Res* 477: 80-90.
- 2.15. Gascoyne T, Colls (2019) In vivo wear measurement in a modern total knee arthroplasty with model-based radiostereometric analysis. *Bone & Joint Journal* 101-B: 1348-1355.
- 2.16. Silva M, Colls (2002) Average patient walking activity approaches 2 million cycles per year. pedometers under-record walking activity. *The journal of Arthroplasty* 17(6).
- 2.17. Ozer A (2022) Computational wear of knee implant polyethylene insert surface under continuous dynamic loading and posterior tibial slope variation based on cadaver experiments with comparative verification. *BMC Musculoskeletal Disorders* 23: 871.
- 2.18. Heisel C, Colls (2004) Short-term in vivo wear of cross-linked polyethylene. *The Journal of Bone and Joint Surgery*.

- 2.19. Abdelgaied A, Colls (2011) Computational wear prediction of artificial knee joints based on a new wear law and formulation. *Journal of Biomechanics* 44: 1108-1116.
- 2.20. Pecora J, Romero V (2020) Evaluation of Polyethylene Wear in a Brazilian Ultracongruent Knee Prosthesis with a Rotating Platform. *Rev Bras Ortop* 56(1): 42-46.
- 2.21. Soni A (2020) Total Knee Arthroplasty (TKA) Wear Analysis on the Tibial Implant using Finite Element Method Approach. (*IJARESM*) 6(1).
- 2.21.1. Bergmann G, Colls (2014) Standardized Loads Acting in Knee Implants. *PLOS one* 9(1): e86035.
- 2.21.2. Dreyer M, Colls (2022) European Society of Biomechanics S.M. Perren Award 2022: Standardized tibio-femoral implant loads and kinematics. *Journal of Biomechanics* 141: 111171.
- 2.22. Innocenti B, Colls (2014) Development and Validation of a Wear Model to Predict Polyethylene Wear in a Total Knee Arthroplasty: A Finite Element Analysis. *Lubricants* 2(4): 193-205.
- 2.23. De Ruiter L, Colls (2020) The Effects of Cyclic Loading and Motion on the Implant–Cement Interface and Cement Mantle of PEEK and Cobalt-Chromium Femoral Total Knee Arthroplasty Implants: A Preliminary Study. *MDPI. Materials* 13(5): 3323.
- 2.24. Kumar V, Colls (2023) Triboinformatic Modeling of Wear in Total Knee Replacement Implants Using Machine Learning Algorithms. *Journal of Materials and Engineering* 1(3): 97-105.
- 2.25. Fisher J, Colls (2001) Wear of polyethylene in artificial knee joints. *Current Orthopaedics* 15: 399d405.
- 2.26. Fuchs S, Colls (2000) Retropatellar contact characteristics in total knee arthroplasty with and without patellar resurfacing. *International Orthopaedics (SICOT)* 24: 191-193.
- 2.27. Koh Y, et al. (2020) Prediction of wear performance in femoral and tibial conformity in patient-specific cruciate-retaining total knee arthroplasty. *Journal of Orthopaedic Surgery and Research* 15: 24.
- 2.28. Stukenborg-Colsman C, et al. (2002) Tibiofemoral contact stress after total knee arthroplasty. *Acta Orthop Scand* 73 (6): 638-646.
- 2.29. Uvehammer J (2001) Doctoral Thesis. Knee joint kinematics, fixation and function related to joint area design in total knee arthroplasty. *Acta Orthopaedica Scandinavica Supplementum* 72(299): 1-52.
- 2.30. Abdelgaied AA, Fisher J, Jennings L (2022) Understanding the differences in wear testing method standards for total knee replacement. *Journal of the Mechanical Behavior of Biomedical Materials* 132: 105258.
- 2.31. Dai Y, et al. (2014) Increased shape and size offerings of femoral components improve fit during total knee arthroplasty. *Knee Surg Sports Traumatol Arthrosc* 22: 2931-2940.
- 2.32. Fekete G, et al. (2017) Tibiofemoral wear in standard and non-standard squat: implication for total knee arthroplasty. *Muscles, Ligaments and Tendons Journal* 7(4): 520-528.

### 3. Numeration-References Biotribology Further Reading and Author's Hip Arthroplasty References

- 3.1. Casesnoves F (2021) Multiobjective Optimization for Ceramic Hip Arthroplasty with Medical Physics Applications. *Int J Sci Res Comput Sci Eng Inf Technol* 7: 582-598.
- 3.2. Casesnoves F (2021) Mathematical Multiobjective Optimization for Metal Hip Arthroplasty with Medical Physics Applications. *Journal of Bioscience & Biomedical Engineering* 2(4).
- 3.3. Casesnoves F (2021) Review of Wear Model Optimization for Ceramic and Metal Total Hip Arthroplasty with Medical Physics Applications. *Current Trends Biomedical Eng & Biosci* 20(2): 556035.
- 3.4. Casesnoves F (2022) Genetic Algorithm to Inverse Least Squares Comparative Dual Optimization for Ceramic Hip Arthroplasty in Medical Physics. *International Journal of Scientific Research in Computer Science Engineering and Information Technology* 8(1).
- 3.5. Casesnoves F (2021) Mathematical Standard-Parameters Dual Optimization for Metal Hip Arthroplasty Wear Modelling with Medical Physics Applications. *Standards* 1(1): 53-66.
- 3.6. Casesnoves F (2018) Nonlinear comparative optimization for biomaterials wear in artificial implants technology. *Applied Chemistry and Materials Science RTU2018 Conference Proceedings Riga Latvia* pp. 52-59.
- 3.7. Merola M, Affatato S (2019) Materials for Hip Prostheses: A Review of Wear and Loading Considerations. *Materials* 12(3): 495.
- 3.8. Navarro N (2008) Biomaterials in orthopaedics. *J R Soc Interface* 5: 1137-1158.
- 3.9. Kurtz S (2014) Advances in Zirconia Toughened Alumina Biomaterials for Total Joint Replacement. *J Mech Behav Biomed Mater* 31: 107-116.
- 3.10. Sachin G, Mankar A, Bhalerao Y (2016) Biomaterials in Hip Joint Replacement. *Int J Mater Sci Eng* 4: 113-125.
- 3.11. Li Y, Yang C, Zhao H, Qu S, Li X, et al. (2014) New Developments of Ti-Based Alloys for Biomedical Applications. *Materials* 7: 1709-1800.
- 3.12. Kolli R, Devaraj A (2018) A Review of Metastable Beta Titanium Alloys. *Metals* 8(7): 506.
- 3.13. Holzwarth U, Cotogno G (2012) Total Hip Arthroplasty. *JRC Scientific and Policy Reports; European Commission: Brussels, Belgium.*

- 3.14. Delimar D (2018) Femoral head wear and metallosis caused by damaged titanium porous coating after primary metal-on-polyethylene total hip arthroplasty: A case report. *Croat Med J* 59: 253-257.
- 3.15. Zhang M, Fan Y (2015) *Computational Biomechanics of the Musculoskeletal System*. CRC Press: Boca Raton FL USA.
- 3.16. Dreinhöfer K, Dieppe P, Günther K, Puhl WE (2009) *Health Technology Assessment of Hip Arthroplasty in Europe*. Springer: Berlin/Heidelberg.
- 3.17. Casesnoves F (2018) 2D computational-numerical hardness comparison between Fe-based hardfacing with WC-Co reinforcements for Integral-Differential modelling. *Trans Tech* 762: 330-338.
- 3.18. Hutchings I, Shipway P (2017) *Tribology Friction and Wear of Engineering Materials*, 2nd ed Elsevier: Amsterdam The Netherlands.
- 3.19. Shen X, Lei C, Li R (2010) Numerical Simulation of Sliding Wear Based on Archard Model. *Proceedings of the 2010 International Conference on Mechanic Automation and Control Engineering Wuhan China* pp.26-28.
- 3.20. Affatato S, Brando D (2009) *Introduction to Wear Phenomena of Orthopaedic Implants*. Woodhead Publishing: Sawston UK.
- 3.21. Matsoukas G, Kim Y (2009) Design Optimization of a Total Hip Prosthesis for Wear Reduction. *J Biomech Eng* 131(5): 051003.
- 3.22. Casesnoves F, Antonov M, Kulo P (2016) Mathematical models for erosion and corrosion in power plants. A review of applicable modelling optimization techniques. In *Proceedings of RUTCON2016 Power Engineering Conference Riga Latvia*.
- 3.23. Galante J, Rostoker W (2014) Wear in Total Hip Prostheses. *Acta Orthop Scand* 43: 1-46.
- 3.24. Mattei L, DiPuccio F, Piccigallo B, Ciulli E (2011) Lubrication and wear modelling of artificial hip joints: A review. *Tribol Int* 44: 532-549.
- 3.25. Jennings L (2012) Enhancing the safety and reliability of joint replacement implants. *Orthop. Trauma* 26: 246-252.
- 3.26. Casesnoves F (2019) *Die Numerische Reuleaux-Methode. Rechnerische und Dynamische Grundlagen mit Anwendungen (Erster Teil)*. Scientia Scripts.
- 3.27. Kulu P, Casesnoves F, Tarbe R (2017) Prediction of abrasive impact wear of composite hardfacings. *Solid State Phenomena*. In *Proceedings of the 26th International Baltic Conference on Materials Engineering*, Trans Tech Publications: Bäch, Switzerland 267: 201-206.
- 3.28. Casesnoves F (2018) *Mathematical Models and Optimization of Erosion and Corrosion* Ph D Thesis Taltech University Evaluated as excellent Tallinn Estonia.
- 3.29. Saifuddin A, Blease S, Macsweeney E (2003) Axial loaded MRI of the lumbar spine. *Clin Radiol* 58: 661-671.
- 3.30. Damm P (2014) *Loading of Total Hip Joint Replacements*. Ph D Thesis Technischen Universität Berlin.
- 3.31. Casesnoves F (2019) *The Numerical Reuleaux Method, a Computational and Dynamical Base with Applications*. First Part Lambert Academic Publishing: Republic of Moldava.
- 3.32. Casesnoves F (2007) *Large-Scale Matlab Optimization Toolbox (MOT) Computing Methods in Radiotherapy Inverse Treatment Planning*. High Performance Computing Meeting; Nottingham University: Nottingham, UK.
- 3.33. Casesnoves F (2007) A Monte-Carlo Optimization method for the movement analysis of pseudo-rigid bodies. In *Proceedings of the 10th SIAM Conference in Geometric Design and Computing San Antonio TX USA*.
- 3.34. Casesnoves F (2021) Theory and Primary Computational Simulations of the Numerical Reuleaux Method (NRM). *Int J Math Computation* 13: 89-111.
- 3.35. Casesnoves F (2021) Applied Inverse Methods for Optimal Geometrical-Mechanical Deformation of Lumbar artificial Disks/Implants with Numerical Reuleaux Method. 2D Comparative Simulations and Formulation. *Comput Sci Appl* 2: 1-10.
- 3.36. Casesnoves F (2018) Inverse methods and Integral-Differential model demonstration for optimal mechanical operation of power plants-numerical graphical optimization for second generation of tribology models. *Electr Control Commun Eng* 14: 39-50.
- 3.37. Casesnoves F, Surzhenkov A (2017) Inverse methods for computational simulations and optimization of erosion models in power plants. In *Proceedings of the IEEE Proceedings of RUTCON2017 Power Engineering Conference Riga Latvia*.
- 3.38. Abramowitz S (1972) *Handbook of Mathematical Functions Appl Math Ser* pp. 55.
- 3.39. Luenberger G (2005) *Linear and Nonlinear Programming*, 4th ed Springer: Berlin/Heidelberg.
- 3.40. Casesnoves F (2016) Exact Integral Equation Determination with 3D Wedge Filter Convolution Factor Solution in Radiotherapy. Series of Computational-Programming 2D-3D Dosimetry Simulations. *Int J Sci Res Sci Eng Technol* 2: 699-715.
- 3.41. Panjabi M, White A (1980) *Clinical Biomechanics of the Spine*. Lippincott 42: S3.
- 3.42. Casesnoves F (2021) Software Programming with Lumbar Spine Cadaveric Specimens for Computational Biomedical Applications. *Int J Sci Res Comput Sci Eng Inf Technol* 7: 7-13.
- 3.43. Surzhenkov A, Viljus M, Tarbe R, Saarna M, Casesnoves F (2017) Wear resistance and mechanisms of composite hardfacings atabrasive impact erosion wear. *J Phys* 843: 012060.
- 3.44. Casesnoves F (2012) Computational Simulations of Vertebral Body for Optimal Instrumentation Design. *ASME J Med Devices* 6(2): 021014.
- 3.45. Barker P (2014) The effect of applying tension to the lumbar fasciae on segmental flexion and extension. In *Proceedings of the 5<sup>th</sup> International Congress of Low Back and Pelvic Pain Melbourne Australia* 10-13 pp. 50-52.

- 3.46. European Textbook on Ethics in Research (2021) European Commission, Directorate-General for Research. Unit L3. Governance and Ethics. European Research Area. Science and Society. EUR 24452 EN.
- 3.47. ALLEA (2017) The European Code of Conduct for Research Integrity Revised ed. ALLEA: Berlin Germany.
- 3.48. Swedish Research Council (2017) Good Research Practice. Swedish Research Council: Stockholm Sweden.



This work is licensed under Creative Commons Attribution 4.0 License  
DOI: [10.19080/APBJ.2025.08.555735](https://doi.org/10.19080/APBJ.2025.08.555735)

### Your next submission with Juniper Publishers will reach you the below assets

- Quality Editorial service
- Swift Peer Review
- Reprints availability
- E-prints Service
- Manuscript Podcast for convenient understanding
- Global attainment for your research
- Manuscript accessibility in different formats  
( Pdf, E-pub, Full TPxt, Audio)
- Unceasing customer service

### Track the below URL for one-step submission

<https://juniperpublishers.com/online-submission.php>